MASTER'S THESIS

Implementation and Testing of SOLID Space Debris Detector for TechnoSat Satellite

Nazmus Sakib
2016

Master of Science (120 credits)
Space Engineering - Space Master

Luleå University of Technology
Department of Computer Science, Electrical and Space Engineering

LULEÅ UNIVERSITY OF TECHNOLOGY

Julius Maximilian University of Würzburg

Faculty of Mathematics and Computer Science

Aerospace Information Technology

Chair of Computer Science VIII

Master Thesis

IMPLEMENTATION AND TESTING OF SOLID SPACE DEBRIS DETECTOR FOR TECHNOSAT SATELLITE

Thesis submitted for partial fulfillment of the requirements for the Degree of Master in Space Science & Technology.

Submitted by

Nazmus Sakib

Matrikel No: 1911156

Examiner and Supervisor: Prof. Dr. Sergio Montenegro

External Examiner: Dr. Anita Enmark

Würzburg

4th April, 2016

Submitted To:

Professor Dr. Sergio Montenegro

Examiner and Supervisor

Informatik VIII

Julius Maximillian Universität Würzburg, Germany

Dr. Anita Enmark

Examiner

Lulea University of Technology, Sweden.

ACKNOWLEDGEMENT

I would like to Thank first of all to **Professor Dr. Sergio Montenegro** for giving me the opportunity to work with the TechnoSat satellite project and being my Supervisor and Examinar. A lot of credit goes to **Atheel Redah** for helping me out with the embedded systems and Real Time operating systems under Linux environment. I would also like to thank the people in DLR and TU berlin for their cooperation and updated information whenever there were changes to the hardware electronics. And, finally **Dr. Anita Enmark**, for her time and consent to be my second examiner.

Abstract

With the increase in numbers of Space Exploration, the Earth's Orbit is now become populated with Man-made debris. This increased amount of Debris have imposed threats to newer space missions. Although, Remote detection Techniques of space debris and putting them into catalogues can help avoiding Spacecrafts with major collisions, the smallest and undetectable particles are of constant threats for both future current and missions. In situ measurements is the only option remained to detect and map those smaller pieces of chunks orbiting with the same speed as other spacecrafts. The Technosat Satellite is a NanoSatellite developed by DLR Bremen and TU Berlin has a secondary goal to fly SOLID instrument in order to detect in situ Particle Impacts. The aim of this thesis work is to implement the and Test the SOLID instruments working principle by means of interfacing, prototype testing and generating simulated results to visualize the impact details on Ground.

Table of Contents

List of Figures:

List of Tables:

1. Introduction:

Years later the SPUTNIK was placed in orbit, the picture of earth orbiting artificial satellites started to change generating more and more population up above. Before the first collision took place, very little did the Space fairing Nations worry about the future of orbital population and the threats associated to them. Today the Major Space Organizations across the world have their own database of detectable space debris and helping others by providing the updated debris catalogs with time. Even though these catalogs are quite rich with the aid of Ground or Space based Telescope observations and Thermal and Infra-red sensing, they are limited down to centimeter sized objects. Still millimeter ranged objects comes in to concerns in LEO. A good solution is to send some retrievable hardware to detect the impacts or in other words in-situ experiments. SOLID (Solar Generated Impact detector) is a secondary payload on a Nanosatellite (TechnoSat) aiming to detect the impacts and map them. TechnoSat is a Nanosatellite from TU Berlin and SOLID hardware was developed in DLR (German Aerospace Center). In this thesis work, the current situation of Space Debris has been presented and importance has been given on: in-situ measurements. Later on the Solid Hardware electronics has been discussed and the hardware interfacing was implemented. Test Cases have been generated using the prototype electronics and Telemetry data. Finally a GUI (Graphical User Interface) has been built in order to simulate the impact conditions in orbit for ground visualization and continuous updates of the Debris mapping.

2. Technical details:

2.1.1 Gravity:

It is ‘Gravity’ that tends to pull every single object down to the center of Earth. Because of Earth’s Gravitational field and pull, we need a rocket with appropriate speed and direction; in other words with a minimum velocity in order to place something in the orbit. Once an object for example, a satellite is placed in the orbit, a certain velocity needs to be maintained to keep it moving around the Earth. With too little velocity than the required amount, the satellite will reenter to Earth’s atmosphere and eventually surrender itself to a free fall trajectory due to the pull of gravity. Again a little bit too much velocity applied to the satellite will cause a change to its orbit. In some cases the object might escape completely from the Earth’s gravity. In order to achieve a specific orbit; in other words, a specific orbital altitude, a satellite needs a proper velocity to maintain over time. However, the satellites orbit changes over time. One of the main reason is due to the fact that, the Earth is not a perfect sphere and the gravitational pull of earth varies at different orbits. Also the asymmetrical shape of Earth and the variation of its own gravitational field creates perturbations on an object that is placed in the orbit. Of course Earth’s gravitational field itself is not the end of concerns; together with the field forces from the Sun, the Moon and other bigger planets (Jupiter), this perturbations can be quite complicated. This is better explained with the N-Body problem. Finally gravitational field of Earth becomes to a smaller concern as the distance increases from Geo Center.

2.1.2 Atmospheric Drag and Earth’s Magnetic field:

The actual orbital altitude of Earth starts from 100 km. even though evidence has been found that the lowest orbital altitude a satellite was flown; was 96 km above the see level [1]. Although NASA defines LEO to start from 100km, most of the realistic LEO satellite mission fly sort of 300 km or above to avoid severe Atmospheric drag, which even continues up to several hundreds of kilometers or even up to a thousand kilometers.

Earth’s atmosphere constitutes of different molecules of gases, those have a greater impact on a satellite travelling at about 8km/s in the orbit. The cross sectional area of the satellites comes into a great contrast to the direction of its velocity and collides with the atmospheric particles. The impact of these Neutral molecules of gasses will transfer some energy and momentum to the satellite cross section that is comes in contact with. The satellite on the other hand, sees these energy and momentum transfers as an exchange in terms of Drag force [2]. Most satellites

placed in the orbital altitude between 150km to 1,000km will encounter this Drag force in Maximum. The Drag at those low height orbits certainly limits the satellite's Lifetime, on board fuel consumption, orbital parameters and momentum dumping from the MWs. A significant amount of on propellant is required on board a LEO satellite to change its orbit over the lifetime. One major example is the ISS; on board ISS there is about 4 tons of fuel to fire some small rocket engines those in turns will generate the required velocity increment for the entire ISS module as its orbit slowly decays over time. Drag can also be a factor of benefit. Natural Drag force can cause a slow reentry of the satellite to Earth's lower atmosphere and causes in atmosphere burn. Which is a very slow but Natural and effective disposal of space chunks from LEO [3].

In orbit satellites are also subject to disturbances by Earth's geomagnetic field. The on board electronics of a satellite produces a magnetic field due to the Earth's magnetic field and produces a small torque. Even though the effect of Earth's magnetic field decreases as the altitude increases, such a small torque causes phenomenal orbit perturbations for LEO satellites.

2.1.3 The radiation Environment:

The radiation environment around the Earth is mainly composed with high energy electrons and protons. Where the high energy electrons have an energy over 100KeV and protons with energies with a minimum of 1MeV [4]. The radiation environment is discussed in three main categories; the Van Allen radiation belt, The Galactic Cosmic Rays (GCRs) and Solar Proton Events (SPE).

Around the Earth, near to the Equatorial altitude, there is a toroid shaped (some say Donought shaped) belt consists of trapped energetic protons and electrons with a trace of heavy ions such as O+. This Toroid belt has two zones: the inner belt or the low altitude segment and the outer belt or the high altitude radiation zone. The inner belts starts from 100km altitude above the sea level near the Equator and extends up to 6000km. this inner belt is mainly contains plenty of trapped energetic protons of Energies ranging from 1-10MeV. Outer Van Allen belt is populated by huge amount of energetic electrons as the main constituent and expanding up to 60,000km in altitude. The region between the two belts contains few energetic particles. Peaking near the equatorial latitude, the strength of the radiation decreases as the altitude rises towards the poles. Van Allen radiation belt has a greater impact on LEO satellites, especially

over the South Atlantic region where Earth's magnetic field becomes weaker. Appropriate shielding is required for LEO satellites in order to protect the on board Electronics.

Interplanetary protons and heavy but ionized nuclei those are associated with higher energies (up to 10^{10} eV) are classified as GCRs. The origin of these particles are galactic and extra galactic. Experiments suggests the distribution of these particles are isotropic outside the Magnetosphere of Earth but non isotropic inside the Earth's magnetosphere. LEO satellites benefit from the cancellation of the GCRs by the Earth's magnetosphere, but still there are chances for the satellites to be affected by Ionized Radiation Dose if the particles penetrate with increased energy. Near the poles, the GCRs can enter nearly in parallel to the Earth's magnetic field lines, hence, PEO satellites are heavily exposed to ionized heavy particles.

During the high solar activities, the sun ejects Coronal mass, which is also referred to solar flares. The solar flares contains high energy protons and other heavy ions. Since the major constituents of solar flares are protons, it is also called as the Solar Proton Events or SPEs. Unlike GCRs, in the case of SPEs, the ejected particles are in very high energetic states (up to 1GeV/nucleon). These particles are responsible for a very harsh changes on digital microelectronics onboard the satellites named as Single Event Upset (SEU). SEU changes the regular behavior of an electronics on board the satellite. In some cases when the particles are associated with enough energy, they can cause the electronics to a completely failure state, leaving the satellite of no use in the orbit. [4].

2.1.4 Space Plasma:

A satellite in orbit can be considered as an isolated probe dipped in to the space plasma. The satellite will eventually start to gather the charged particles from the plasma and in some cases also releasing some of the charges from the satellite body. This exchange of charges will bring the satellite in an electrically charged state; meaning, the satellite being charges either negatively or positively. This phenomenon is generally known as spacecraft charging. In GEO, the satellite is exposed at the very edge of the Earth's plasma sphere and the chances for a GEO satellite is quite obvious to be charged due to the Space plasma. The Debye length in GEO is much bigger than the satellite dimension, and the plasma in GEO can be thought of as a collection of isolated charged particles. Spacecraft charging in GEO is quite common and does not affect the operation of the satellite. However, there is another type of spacecraft charging, which involves deposition of high energy electrons inside the satellite body and can cause

breakdown of high voltage insulators. LEO satellites are also exposed to the plasma flow in orbit and eventually the satellite gets electrically charged up. Unlike GEO, the Debye length in LEO is smaller than the satellite dimension and the LEO plasma is characterized as collisional plasma. LEO satellite exposed to plasma or neutral flow is complicated to analyze, but in both cases similar approaches are taken to prevent undesired events in the orbit, for example: spacecraft EMI test on ground.

2.1.5 Macroscopic Particle Environment:

Macroscopic particles are common around the orbits of Earth or around another planet in our solar system: Saturn for example. Whatever the particles are made of, they pose a greater threat to satellites due to their extraordinary velocity, distribution in a specific orbit or even the sizes. Small space chunks irrespective of their origin, can damage satellite surface structure or even internal components. The natural way of having these particles gathered around a planet is from the sources of Comets, Asteroids, and Meteoroids etc. Saturn's ring for example is made of these natural particles. Of course they are ice particles of different dimensions and masses. These particles create new particles when they collide to each other. Sometimes they combine together to form a bigger chunk under optimum pressure and temperature.

The second way is rather artificial or manmade activities in the space that creates particles of different sizes and masses. The common reason are remaining fragments from rockets, rocket thrusters or boosters, dead satellites, paint chips came off a satellite structure or rocket body. Since the exploration in orbit by a satellite has been increased significantly over the last couple of decades, the near Earth orbits are quite crowded now. Sometimes, these artificial debris work in a 'Chain reaction' fashion. Old debris collide with new satellites and creates more new chunks, the population increases, so does the probability for a satellite getting hit by another impact. In the upcoming sections a detailed description of debris and mitigation techniques will be discussed.

2.2 The Earth's orbits:

Depending on the orbital height, or in other words, the distance between the satellite and the Geo Center, a satellite experiences faster or slower motion around Earth's orbit. The closer the satellite is to Earth, the stronger is the gravitational pull and the satellite moves in a higher

velocity in order to cancel out the inner pull and to stay in the orbit. The orbital height also plays an important role determinant for naming the orbit. There are mainly three different kinds of orbits: Low Earth Orbit (LEO), Medium Earth Orbit (MEO) and the Geosynchronous Earth Orbit (GEO). The different types of orbit has its own benefits. The most common in use are the LEO and GEO, hence the threat to satellite in either orbit is quite high. Telecommunications and Digital Video Broadcasting, IP over satellite has increased the demand for GEOs and earth observations and universities and scientific organizations who wants to experiment new technologies in microgravity conditions, are vastly dependent on LEOs. Over the years, these two zones are ever congested due to the increasing demand to place a satellite in those particular orbit.

2.2.1 Low Earth Orbit (LEO):

According to NASA, the LEO starts from 100km or above and can limits at around 1000km. in LEO the satellite is quite closer to Earth and so to the pull of gravity. To balance the motion in orbit, the satellite demands greater velocity; 7-8 km/s. all the scientific satellites and NASA's Earth observation satellites are placed in LEO. The advantage of LEO is a shorter orbital period and more overpasses. This switches on the chance for revisiting particular regions on earth from overhead. Typical LEO satellites have an orbital period between 80-110 min and the altitude is between 500km -1000km. For example, NASA's Aqua satellite orbits at 705km altitude and requires 99 min for a complete pass around the Globe.

2.2.2 Polar Orbit (PO):

Polar orbit is a special case of LEO, where a satellite's orbital inclination is nearly close to the latitude of the poles i.e. 85°-105°. The first one with 85° inclination will follow a Prograde or direct motion and the later one will follow a retrograde motion or reverse motion. In this kind of highly inclined orbit, the satellite moves from pole to pole and observes the Earth's surface underneath. Typical orbital period for a PO satellite would be around 90-120 minutes. During 24 hours, a Polar satellite will get to see most of the places on Earth's surface twice; one in daylight and the other in the Dark.

2.2.3 Sun Synchronous Orbit (SSO):

A special case of PO is a Sun-synchronous orbit. Such an orbit is a so called 'Sweet Spot' for polar orbiting satellites. As the earth rotates about 0.98° around the orbit of Sun, we have a change of sun Angle on the Earth. This shift can be compensated by rotating the orbital plane

of a PO satellite by the same angle. The main advantage of Sun-synchronous orbit, is the local Sidereal Time (LST) matches exactly whenever the satellite passes over a region on Earth. Even though the sun angle to earth changes over the year, SSO ensures consistent sunlight on a particular footprint on Earth's surface. Such an orbit is very essential when we want to gather data for a particular region over years in all seasons and almost every clock time. That means, without biting our nails, we are able to gather huge data over the time, which is impossible without SSO.

Since Sun-synchronous orbit is very exact in case of LST for a particular location, a slight change in one of the orbital parameters (inclination, argument of perigee or even orbital altitude) will cause mismatch to the LST and overpass. If a SSO satellite has an orbital altitude of 100km, the orbital inclination has to be 96°. And to maintain the orbital parameters consistent, SSO satellites need sufficient fuel onboard the satellite to fire thrusters and change the orbital plane [5].

2.2.4 Medium Earth Orbit (MEO):

MEO are sometimes called semi –synchronous orbit, satellite in this orbital altitude (which is about 26,560km from the center of Earth) has an orbital period of 12 hours. So, satellites in this orbit will sweep the same spot on Equator twice in every 24 hours; once in day and once at night. MEO satellites have a very lower eccentricity and the shape of orbit is almost circular. Global Positioning System (GPS) uses this kind of Orbit.

2.2.5 Highly Elliptical Orbit (HEO)

Another kind of MEO is called HEO or Molnya Orbit. The Russians invented Molnya orbit for to establish communication Network over the far North and far South. The Molnya orbit also has an orbital period of 12 hours; but the major change is in the orbital inclination (i= 63.4°) and eccentricity (e=0.722). So, a HEO with the above i and e value will become a Molnya Orbit. GEO satellites are the best choices for consistent viewing. Since the GEO satellites are parked over the Equator, the view in its footprint to the far South or far North are limited. This is where Molnya comes into a great use due to its slow pass over the high latitudes to both Hemisphere. Two third of its orbital period, the satellite stays over the higher latitude. The Sirius Radio Satellites also use Molnya Orbit for their satellites [6].

2.2.6 Geostationary orbit (GEO):

At the distance of 36,000km from the surface of Earth something interesting happens. At this height, the satellite rotates around the exactly at the same speed of the Earth's rotational period

on its own axis. The time taken for this is 23 hours, 56 min and 4s. As the satellite rotates as the same rate to the Earth, the satellite views the same spot on the Earth forever, with a little drift to the North and South is to be considered. This orbit is generally called Geo-synchronous orbit.

A Geo-synchronous satellite with zero inclination and i.e. placed overhead Equatorial latitude and zero eccentricity (fully circular orbit) is called as geostationary (GEO) satellite. All modern communication satellites and Meteorological satellites are placed in to the GEO to achieve the constant footprint of the Globe. Three Geo satellite, each placed 120° apart from each other will view the entire earth constantly. Many GEO satellite operators maintain a constellation with minimum three satellites for worldwide coverage.

A slightly higher orbit than GEO is known as the Graveyard orbit. At the end of life, each GEO satellites fire a final thruster and they are transferred to Graveyard orbit. This action makes the corresponding GEO in a particular longitude free and a new GEO satellite is ready to be launched. [5]

2.2.7 Other orbits:

Among the other interesting ‘Sweet spots’, Lagrange point is of very importance. There are 5 main Lagrange points and only two of them (L4 and L5) are stable. Anything placed in either of these two points is like ‘a ball placed in a bowl’, meaning irrespective of the perturbations from the Sun and the Moon, the object will always stay inside the point. The main secret of Lagrange point is the ‘cancellation’ of Earth and Sun’s gravitational pull.

The first Langrange Point (L1) is situated between the Earth and the Sun. this point is its advantage to monitor the Sun constantly. The Solar and Heliospheric Observatory (SOHO) which is a combined Sun Monitoring Project from ESA and NASA, has placed a satellite in L1 point.

The second Lagrange point (L2) is situated at about the same distance from the Earth but on the opposite to the Sun. this leaves the Earth in the middle. Since this point constantly blocks one side from the sunlight, a deep space Astronomical Telescope is an ideal thing to place in L2 as it needs one less heat shield. The James Webb telescope (the successor of HUBBLE) has been placed at this point to map the cosmic microwave background of the entire Universe.

If the Sun, Earth and a spacecraft is placed in a straight line, with sun in the middle, at a particular distance from the Sun's center, it gives L3, the third Lagrange point. A satellite placed in this point is exposed to extreme heat condition, but able to convert more energies from the sunlight. Extreme heat shielding is another challenge for the satellite to survive from the constant exposure of sunlight and CMEs. Even if a satellite is placed at this point, it will eventually not be able to establish any communication with Earth.

Two identical but opposite facing Lagrange points are L4 and L5. Each are the 60° apart from the Sun-Earth line. These two are the most stable Lagrange points and the other three are critically stable and needed to be adjusted in case of perturbations. The Solar terrestrial Relations Observatory (STEREO) will place twin satellites in the fourth and fifth Lagrange points. This will collect 3D images of the sun.

2.2.8 Lunar Orbit:

The moon is orbiting Earth in every 28 days from being at a distance of 384, 403 kilometers from the center of Earth; is the only 'Natural Satellite' of Planet Earth.

2.3 Laws of motion:

2.3.1 Keppler's Laws of motion:

Johann Keppler (1571-1630) in his *Astronomia Nova* (New Astronomy) published his first two laws of planetary motion. The work was published in 1609. Ten years later,the third law of his planetary motion came up a bit later from his own interest of Theological aspiration and was published in his *Harmonices Mundi Libri* (Harmony of the World) [7].

1. The first law of planetary motion states that each planet moves around the Sun in an elliptical orbit; with Sun in one focus of the ellipse.
2. The joining line of a Planet and Sun sweeps out equal area in equal time.
3. The orbital period of a Planet squired is directly proportional to the Mean distance between Sun and the planet cubed. [1]

[1] $T^2 \propto M^3$. Where T is the orbital period and M is the Mean distance between sun and the planet.

2.3.2 Newton's laws of motion:

Even though Keppler's laws of planetary motion were given the shape in its form of Kinematics, they did not receive the shape in form of Dynamics until Sir Isaac Newton came up with his set of rules for laws of motion and published in 1687 in his book *Philosophiae Naturalis principia Mathematica* (Mathematical principles of Natural Philosophy) [7].

1. Every Body tends to conserve its state of rest or to continue its uniform motion in a straight line, unless a force is applied on it to change its state.
2. The change of motion is proportional to the motive force applied to a Body and is made in the direction of a straight line, in which the force is applied.
3. Every action is always opposed by an equal reaction.

2.4 The classical orbital parameters:

There are six classical orbital elements: Semimajor axis (*a*), Eccentricity (*e*), Inclination (*i*), Right Ascension of the Ascending Node or RAAN (Ω), Argument of Perigee (ω) and true anomaly (v). The first two orbital parameters defines the shape and the size of the orbit. Whereas, the other elements completes the orbit description in a reference frame.

The *Semi major axis* is sometimes replaces as *Semiparameter (p)* due to the fact that a parabolic orbit has an infinitely long *semimajor axis*. If a and b are the *semi major* and *semi minor* axis of an orbit, then the following relation is valid:

$$p = \frac{b^2}{a} = b^2(1 - e) \tag{1}$$

The second classical orbital element is *eccentricity (e).* For different conic sections, the eccentricity is different. The relation between the first and second orbital element can be expressed as:

$$e = \sqrt{\frac{p}{a}}\,, h = \sqrt{^2\mu p} \tag{2}$$

A circle has zero eccentricity,$e = 0$, for an elliptical orbit, $e < 1$,

[2] μ is the product of Universal Gravitational Constant and the Mass of Earth.

In a parabolic orbit, $e = 1$ and Hyperbolic orbit comes with $e > 1$

The third orbital parameter defines the tilt of the orbit from the Equator. The amount is measured by the angle between the vector **K** and angular momentum vector **h**. The equatorial orbit has either 0° or 180° inclination. The regular convention for orbits with inclination between 0° and 90° is *direct orbit* [3] and between 91°-180° is *retrograde orbit*[4]. Following relation is used to determine the orbital tilt:

$$i = cos^{-1}\frac{\mathbf{K}\,.\,\mathbf{h}}{|\mathbf{K}||\mathbf{h}|} \tag{3}$$

Right Ascension of Ascending Node (RAAN) is an angle (Ω) in the Equatorial plane, which is measured between **I** vector and the *Ascending Node*. All satellite orbits have both *Ascending*[5] *Nodes* and a *Descending Node*s[6]. The joining line between two *Nodes* is called the *line of Nodes*. There is a vector notation associated to the Nodes, named as Node vector (**n**).The value of RAAN varies between 0° to 360°, according to the right- handed coordinate system; as if seen from the North Pole.

$$\Omega = cos^{-1}\frac{\mathbf{K}\,.\,\mathbf{n}}{|\mathbf{K}||\mathbf{n}|} \tag{4}$$

$$\text{when } (\mathbf{n_J} < 0)\ then\ \Omega = 360° - \Omega$$

$$\text{where } [7]\mathbf{n} = \mathbf{K} \times \mathbf{h} \tag{5}$$

The Argument of Perigee (ω) is another angle measured between the Asscending Node to the *Periapsis or Perigee*[8]. The measure varies between 0° to 360°; however, a perfectly *circular orbit* or *an equatorial orbit* does not have any ω[9]. Argument of Perigee can be obtained from the following formula:

[3] Direction of orbital motion matches with Earth's rotation.
[4] The orbital motion opposes the Earth's motion.
[5] A satellite crosses Ascending Node at the Equator when it travels from Earth's South Pole to the North Pole.
[6] A satellite crosses Descending Node at the Equator when it travels from Earth's North Pole to the South Pole.
[7] Node vector is the cross product between K vector and the angular momentum vector.
[8] Closest distance between a satellite and Earth's center while it's in the orbit.
[9] A circular orbit has null eccentricity vector (**e**) and an Equatorial orbit has null Node vector (**n**).In either case, the dot product of both vectors will always yield a null value.

$$\omega = cos^{-1} \frac{\mathbf{n} \cdot \mathbf{e}}{|\mathbf{n}||\mathbf{e}|} \quad (6)$$

$$\text{If } (\mathbf{e_K} < 0)\ then\ \omega = 360° - \omega.$$

The sixth and the final classical Keplerian orbital element is called True Anomaly which is notated by symbol *v*. This orbital element tells us about the angle between Perigee and the current position vector of the satellite. A dot product between the eccentricity vector and Satellite's position vector is required to find True Anomaly. Mathematically it is expressed in the following form:

$$\nu = cos^{-1} \frac{\mathbf{e} \cdot \mathbf{r}}{|\mathbf{e}||\mathbf{r}|} \quad (7)$$

$$\text{If } (\mathbf{r}.\mathbf{v} < 0)\ then\ \nu = 360° - \nu.$$

2.5 Coordinate Systems:

In order to describe an orbit or a satellite's position in the orbit, we need a coordinate system. There are different coordinated systems in use, depending on the satellite state representation.

2.5.1 Heliocentric Coordinate System:

Interplanetary satellites for example, use a *Heliocentric Coordinate System* with the sun being the origin of the reference frame[10]. The primary and main direction in the XYZ frame is the direction of Vernal Equinox or the First Point of Aries.

2.5.2 Earth or Geocentric Coordinate System:

This is the most common Coordinate System used today to represent an orbit of a satellite. In the XYZ frame, the X direction is the Direction towards the Vernal Equinox. Z axis represents the Northern Celestial Pole and Y axis is the third axis in the Orthogonal Triad according to Right Hand Coordinate System. The origin of this reference frame is the Earth's Center. Today almost all the Earth orbiting satellites uses this coordinate system. The regular nomenclature to this reference frame is Earth Centered Inertial (ECI) or Earth Centered Earth Fixed (ECEF). It

10

is also evident to use Earth's surface on a particular location or even off the Earth's surface as the origin of the Earth based coordinate system.

In an ECI coordinate system, a satellites position and velocity can be easily represented as follows. Here I, J and K are unit vectors for the orthogonal axis.

$$\overrightarrow{r} = \overrightarrow{r_I} + \overrightarrow{r_J} + \overrightarrow{r_K} \text{ and } \overrightarrow{v} = \overrightarrow{v_I} + \overrightarrow{v_J} + \overrightarrow{v_K}$$

2.5.3 Satellite Based Coordinate Systems:

There are mission specific coordinate systems for different satellite mission. Although it is used to describe a particular satellite orbit and the satellites state, it doesn't follow a standard form. So, there are many satellite based systems are available. This system basically uses the true Anomaly and other orbital elements to represent a satellites state in the orbit. [8]

2.6 Coordinate Transformation:

Time to time it is convenient to transform the satellites state from one reference frame to the other. The coordinate transformation is comprised of two main principles, the *rotational transformation* and the *translational transformation*. Translational transformation is comparatively easier as they deal with vector addition and subtraction. However rotational transformation can be quite complicated and involves a lot of mathematics. In case of rotational transformation, the vector will only be changed by its three components but the length and direction of the original vector will remain unchanged. There are different Algorithms for different Coordinate transformations.

3. All about Space Debris:

3.1 What are Space Debris?

Quite often the term *Space Debris* and *Orbital Debris* are used to indicate the same thing. In space the Debris originate from two main sources; *the micrometeorites* from inner and outer solar system and the later one originates from artificial sources i.e. manmade space objects. Either way the Debris puts the satellite in Earth's orbit in to threat. Depending on the size of the Debris, upon collision a satellite can ends up being from partial failure to complete destruction Mode. According to the *Inter-Agency Space Debris Coordination Committee* (IADC), the Space Debris are all non-functional manmade objects orbiting Earth or reentering Earth's Atmosphere including the Fragments and elements [9].

The adopted definition of Space Debris also include the reentry objects those enter into the Earth's Atmosphere and burn up as they go through sever Aerodynamic or Aerothermal heating. It is believed that today almost nearly 60% of the total cataloged space Debris have been decayed due to this phenomenon [9].

As the space Era became more and more popular with the invention of new and powerful Rockets, more and heavier payloads were placed in to the Earth's orbit. This ranges from LEO to GEO and in between. Explosion in orbit created small to big chunks in the orbit and created more and more by colliding with newer payloads in orbit. Sooner the whole process spreaded like a chain reaction. Today the actual picture of manmade Space Debris are quite horrifying and threat for the future space exploration, until and unless Space Agencies and Countries responsible come up with some quick solution to clear up the scenario.

3.1.1 Sizes of Space Debris in Orbit:

Debris have been classified into three major groups; mainly based on their dimension, population, distribution and imposed threats to all other active payloads and spacecrafts orbiting the Earth. The table below gives an estimated population of all cataloged Debris those has been tracked and recorded in the Debris database by different organizations.

- Objects larger than 10 cm in diameter are of greater concerns, as they can be fatal to a satellite as it collides. These group of Debris population can easily be detected by Ground based observations, such as radars or other Optical sources.

- The next group of space chunk fall within the diameter range between 10cm and 1cm. these are also trackable and are cataloged accordingly. However it needs improved sensors techniques.
- Objects smaller than a centimeter diameter are almost impossible to track. Even though NASA JPL and MIT are able to track those small fragments, it needs hundreds of hours of tracking over a year time. The main technique to detect and map the distribution of these fragments is to use in situ experiments. This thesis involves such experiments with an instrument to detect smaller debris and to map their distribution in orbit [10].

Category	Dimension	Potential Threats	Estimated numbers
Trackable	>10cm in Diameter	Complete destruction of satellites	~ over 1900
Potentially Trackable	>1 cm in Diameter	Complete to partial destruction	Several hundred thousands
Untraceable from Ground	< 1cm	Degradation, and loss in subsystems or sensors level	Many millions up to billions.

Table 1: The current Debris scenario.

3.2 Current state of space Debris:

The manmade space environment around the Earth was rather a small picture for about 50 years or so after the first satellite was launched in to the orbit, back in 1957. During that period of time, most of the objects those were released in space were simply the results of launch activities, the deployment of payloads, upper stages of rockets those deployed them in to the space. Some other mission associated objects were also released as part of the launch event, such as: launch adapters, lens covers, clamp bands etc. Some objects were placed I orbit unintentionally. These includes, the screwdrivers, protective gloves of Astronauts as part of their extra vehicular activities in space, paint chips, surface coatings from another spacecraft, slag particles produced as part of rocket booster burning, cooling liquids from some specific

satellites etc. among them the very important first space Debris was formed as a satellite exploded in orbit or the same happened for a upper stage rocket [11].

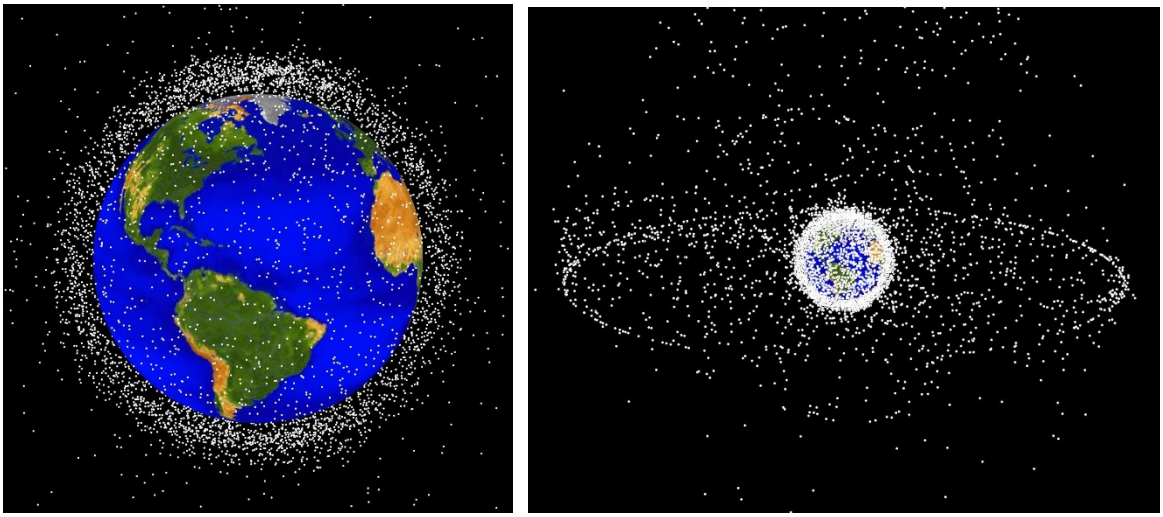

Figure 1: Current Debris densities in LEO and GEO. [Image courtesy: NASA]

To have an understanding about the current space debris environment around Earth, we need a record to look at all the information about trackable objects[11], their origin[12] and their properties. For this a comprehensive data set is constantly provided by NASA Satellite Situation Report (SSN) and formerly known US Space Command. The later organization catalogs the Two-Line Element[13] of trackable objects in Space [11]. They are based on observation data and orbit determination from US Space Surveillance Network (SSN). Even though these data can spot the debris in space, due to the limitations of the Radar and telescope sensitivities, SSN date are good for detecting objects larger than 10cm in diameter in the Low Earth orbit and objects larger than a meter in Geostationary orbit.

The current picture of Cataloged Satellites and Debris are presented in different graphical patterns for better understanding.

[11] Objects those can be observed and classified in terms of their orbits.
[12] Origin of an object in space is associated with the launch.
[13] A convention to represent a satellites state in orbit with the aid of orbital elements.

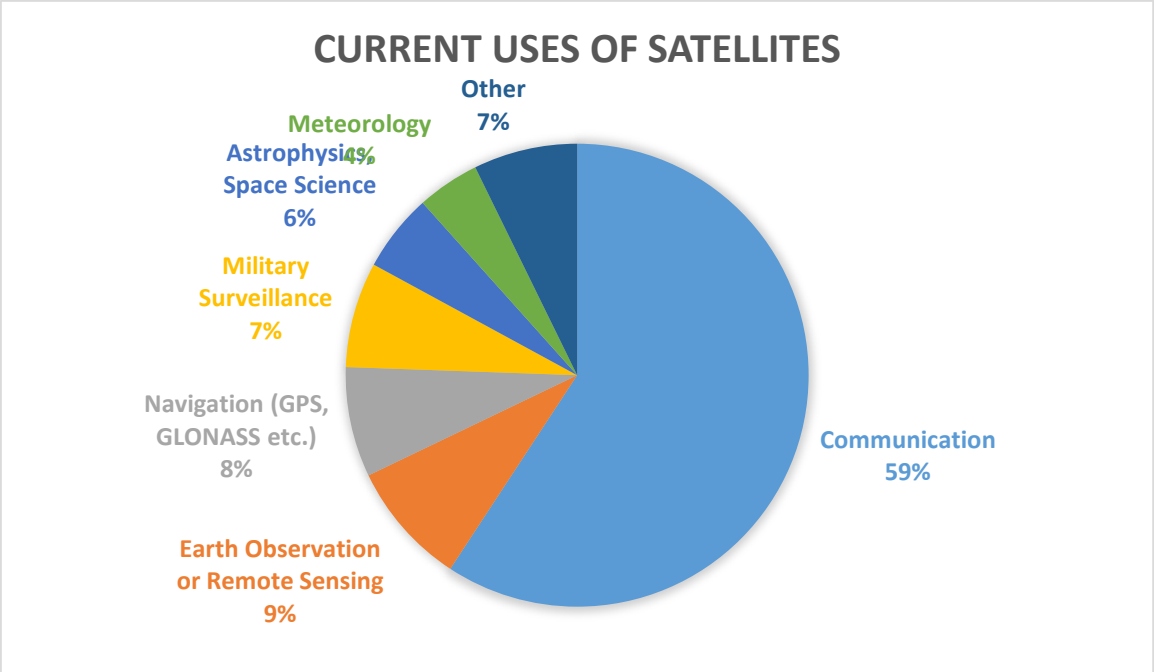

Figure 2: Current occupation of different satellites according to their functionality in orbit. [51]

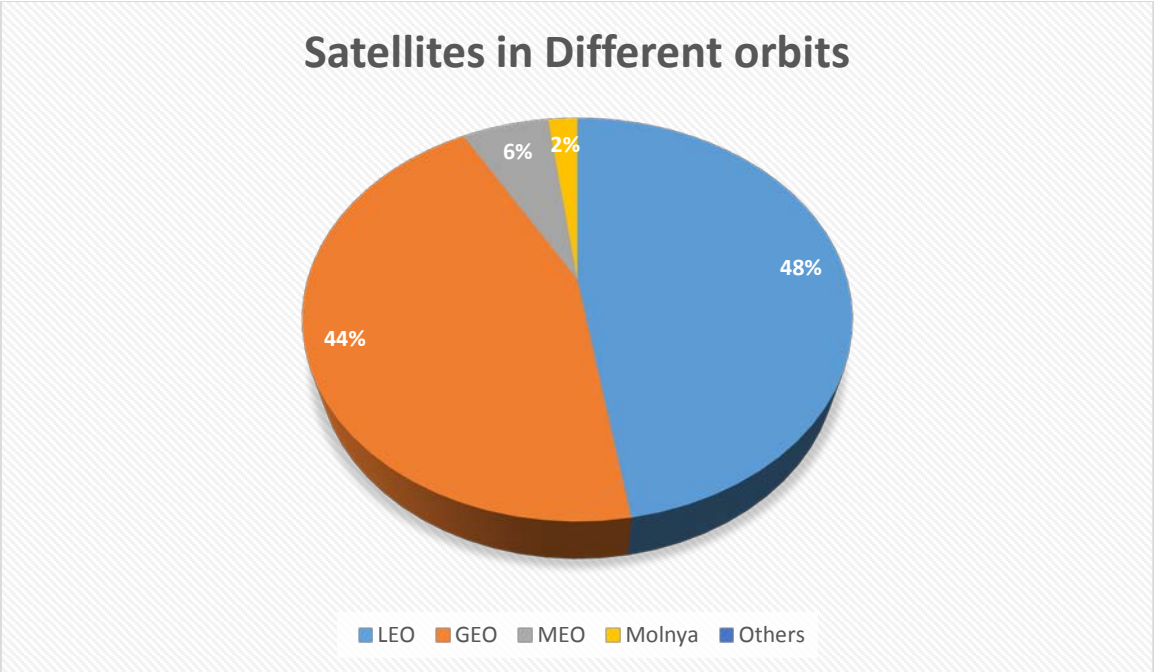

Figure 3: The major satellites in the different orbital heights. [51]

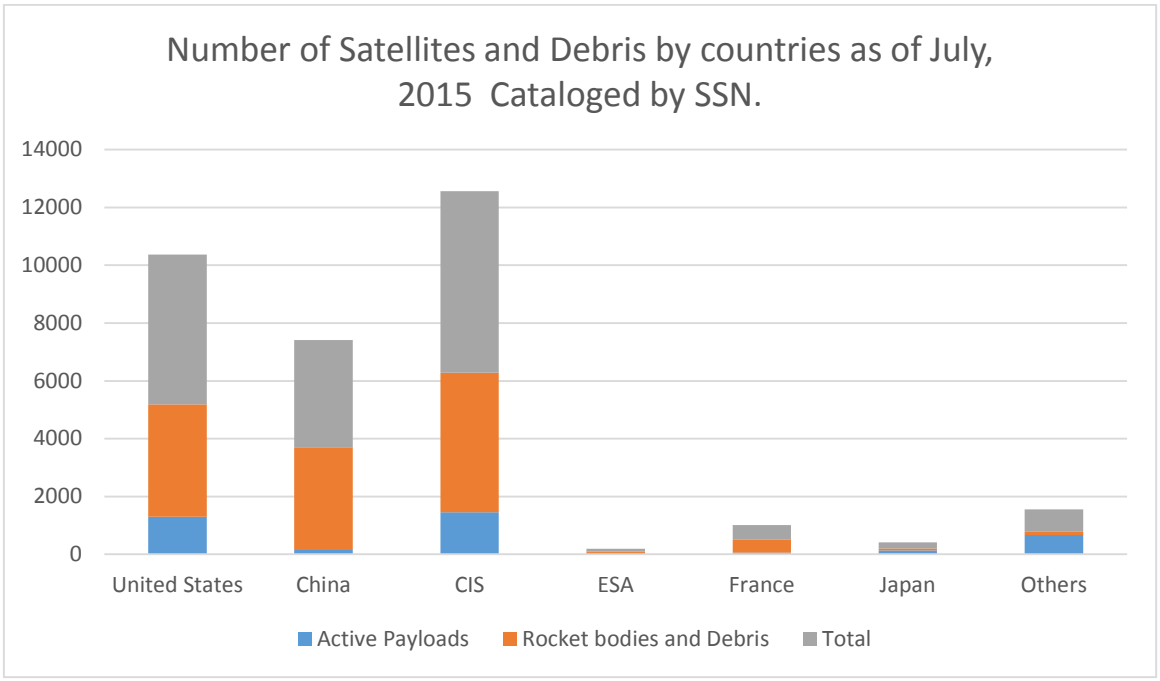

Figure 4: the latest picture of Active payloads and Debris in Space [18]

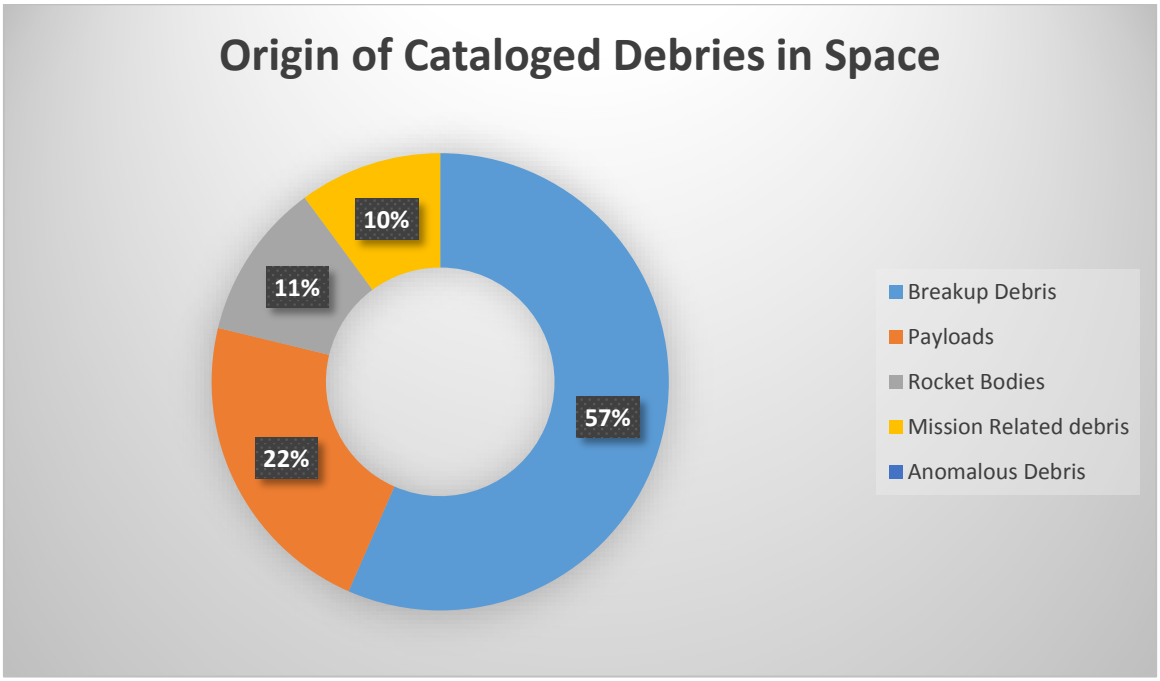

Figure 5: origin of different cataloged debris in space. [51]

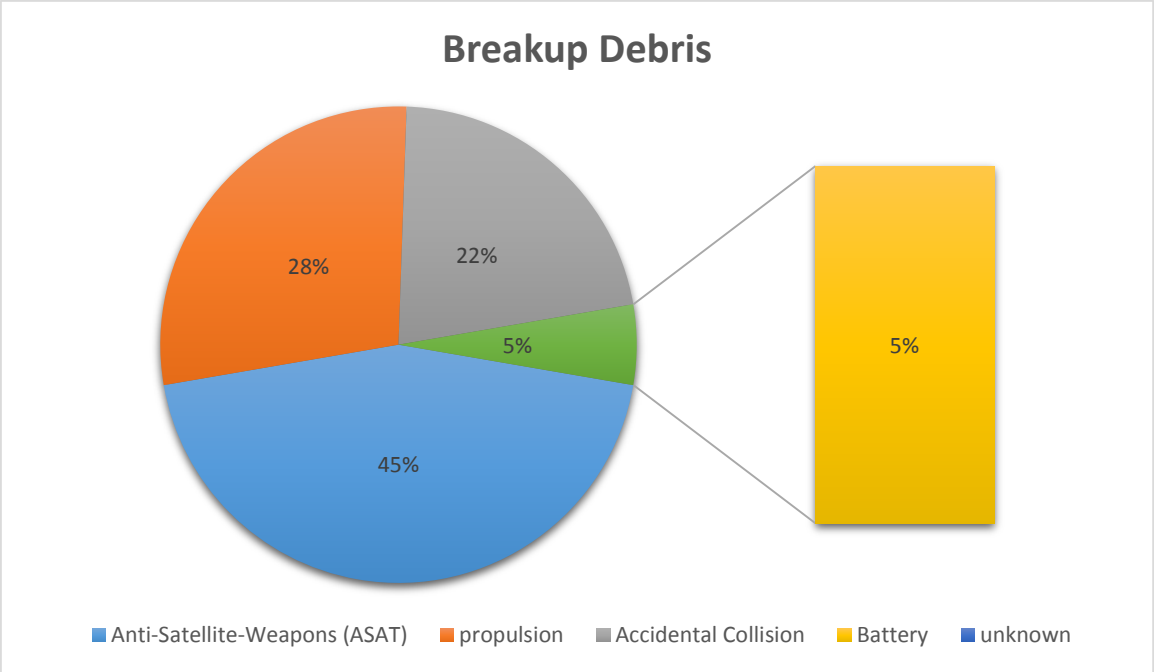

Figure 6: Breakup Debris due to different events. [51]

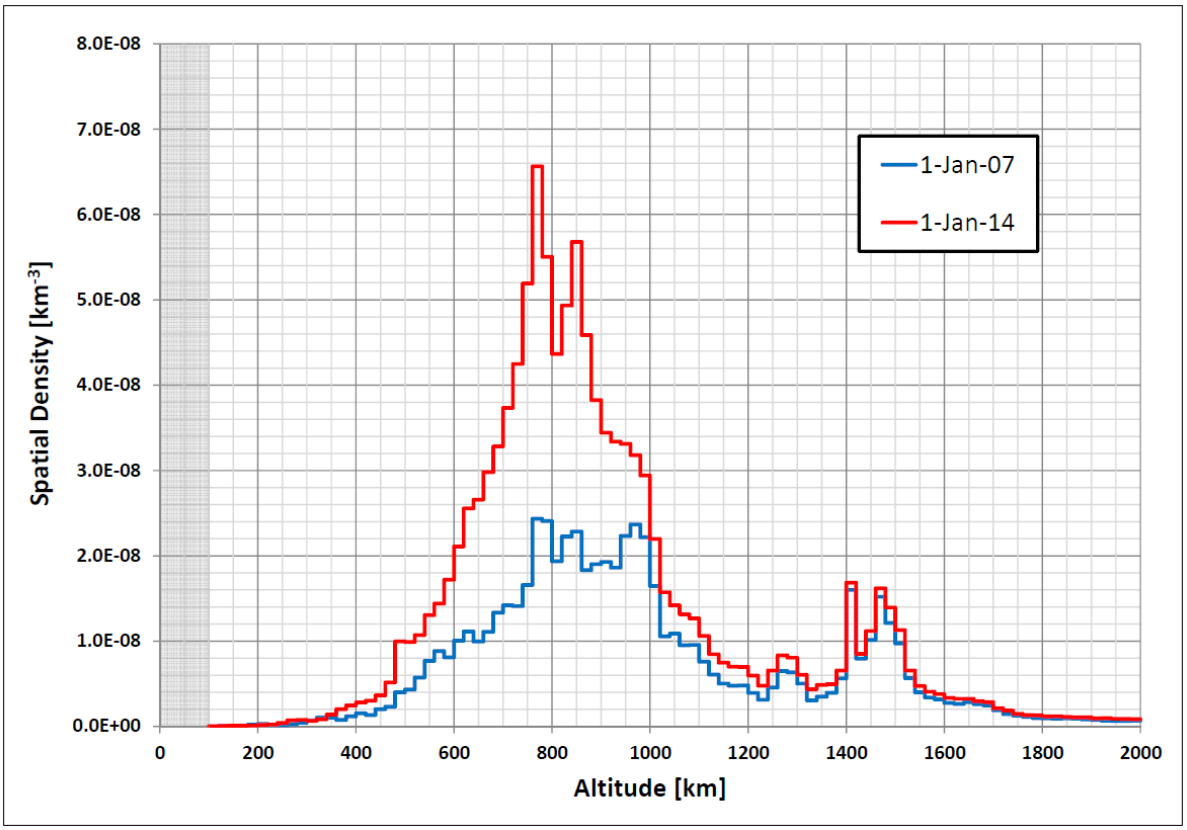

Figure 7: this chart compares the spatial density of Debris in LEO in year 2007 and 2014 [12]

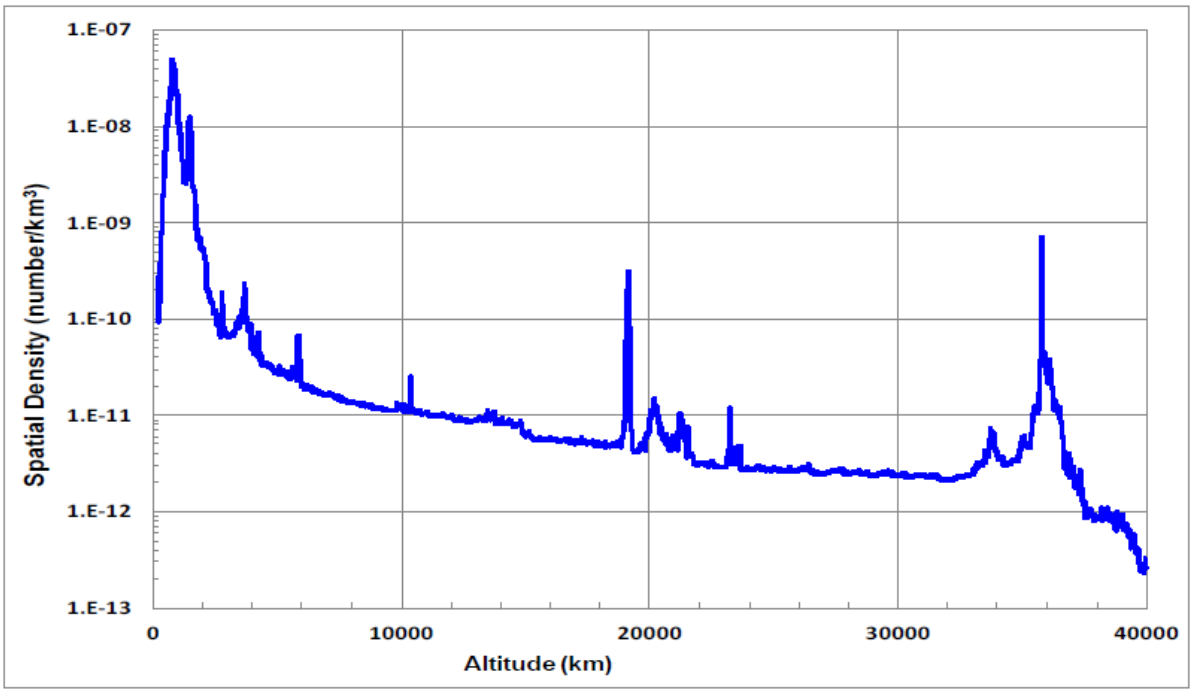

Figure 8: Spatial densities through GEO [image: NASA orbital debris office]

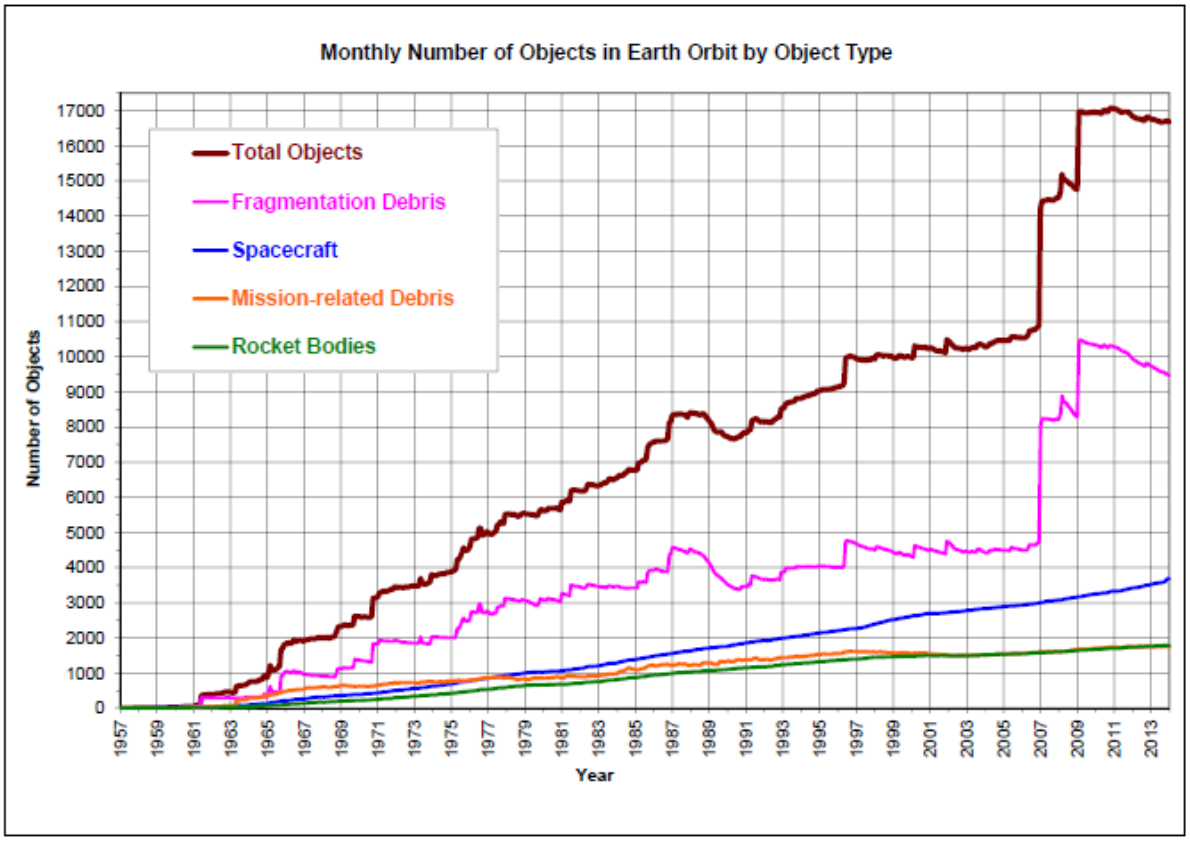

Figure 9: this chart shows the latest official summary of Debris in Earth orbit, cataloged by SSN. [13]

3.3 Consequences of Space Debris:

In the year 2006, the average time between collisions of a debris was something between 5-6 years. Today this risks even higher; one collision event in an average of 2-3 years. The chances for a LEO satellite in the altitude range 800-900 km, satellites are prone to a collisional event by an object greater than a centimeter. This probability is higher than 1% over the satellites 5-10 years lifetime [51].

Although Debris are cataloged these days, there are many uncatalogued debris remains untracked in orbit. The result is unwanted collision with another satellite in orbit, causing a Breakup event and later the process spreads like a chain reaction known as 'Kessler Syndrome'. Collision avoidance maneuvering is only possible if there are cataloged debris in the same satellite orbit. In other cases, the collision is unavoidable. It was stated earlier that objects of millimeter range cannot be tracked and cause partial to subsystem failure to a satellite. Here are some known major in orbit collisions are illustrated:

Year	Event Description
1991	Inactive Cosmos 1934 was hit by catalogued Cosmos 296 satellite.
1996	Active French Cerise satellite hit by catalogued debris from Ariane rocket stage.
1997	Inactive NOAA 7 satellite was hit by uncatalogued debris which was large enough to change the satellite's orbit and create further debris.
2002	Inactive Cosmos 539 satellite hit by uncatalogued debris and the consequence was similar event to that of NOAA 7.
2005	U.S. Rocket body was by a catalogued Chinese Rocket Stage.
2007	Active Meteosat 8 satellite hit by uncatalogued debris leaving the satellite in a changed orbit.
2007	Inactive NASA UARS satellite was hit by uncatalogued object and the event was good enough to create additional debris
2009	Iridium satellite; which was in action, was hit by inactive Cosmos 2251.
2015	Active USA 109 Meteorological satellite experienced a single breakup event.

Table 2: the most common in orbit collisions. Data source: [51]

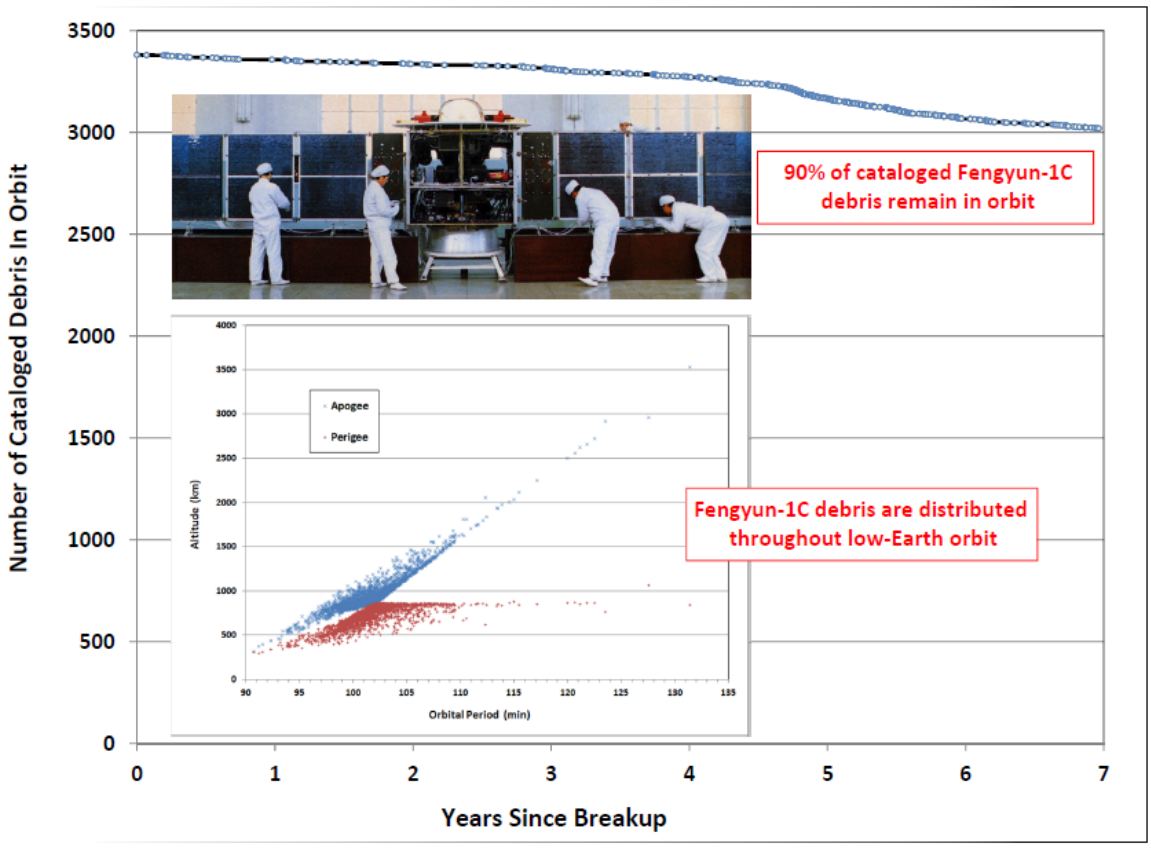

Figure 10: More than 3000 catalogued Debris from Fengyun -1C are in orbit posing threats to spacecraft operations. [13]

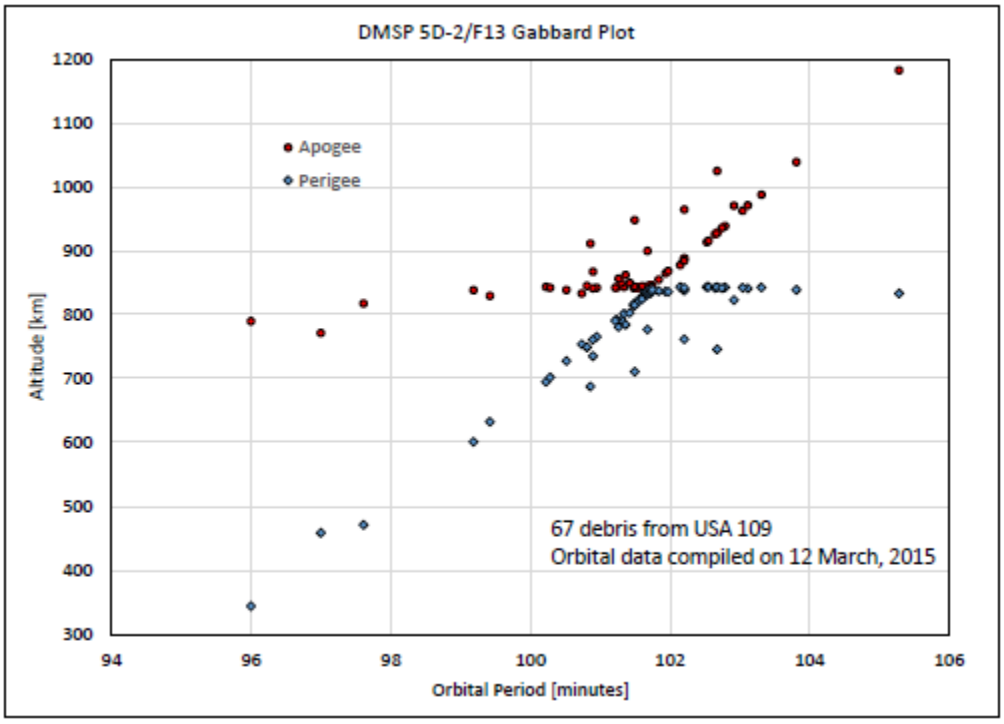

Figure 11: Gabbard plot showing the after breakup dispersion of 67 debris from USA 109 satellite.[14]

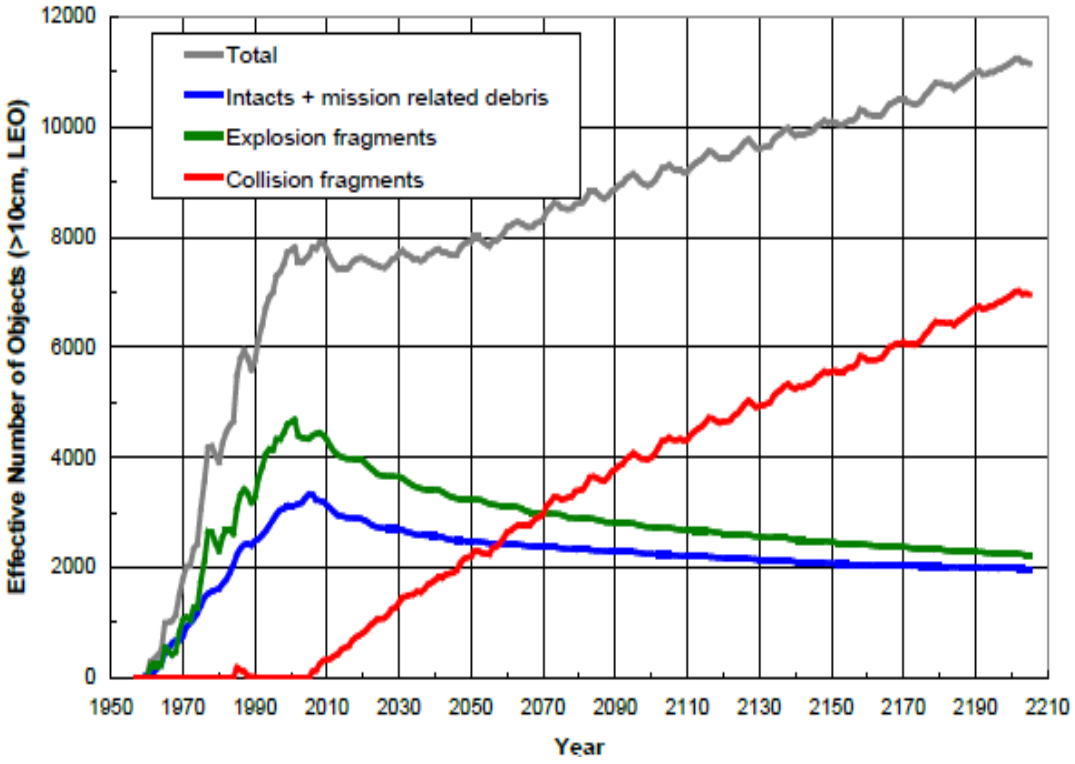

Figure 12: 200 years of debris evolution in LEO (900-1,000km). [52]

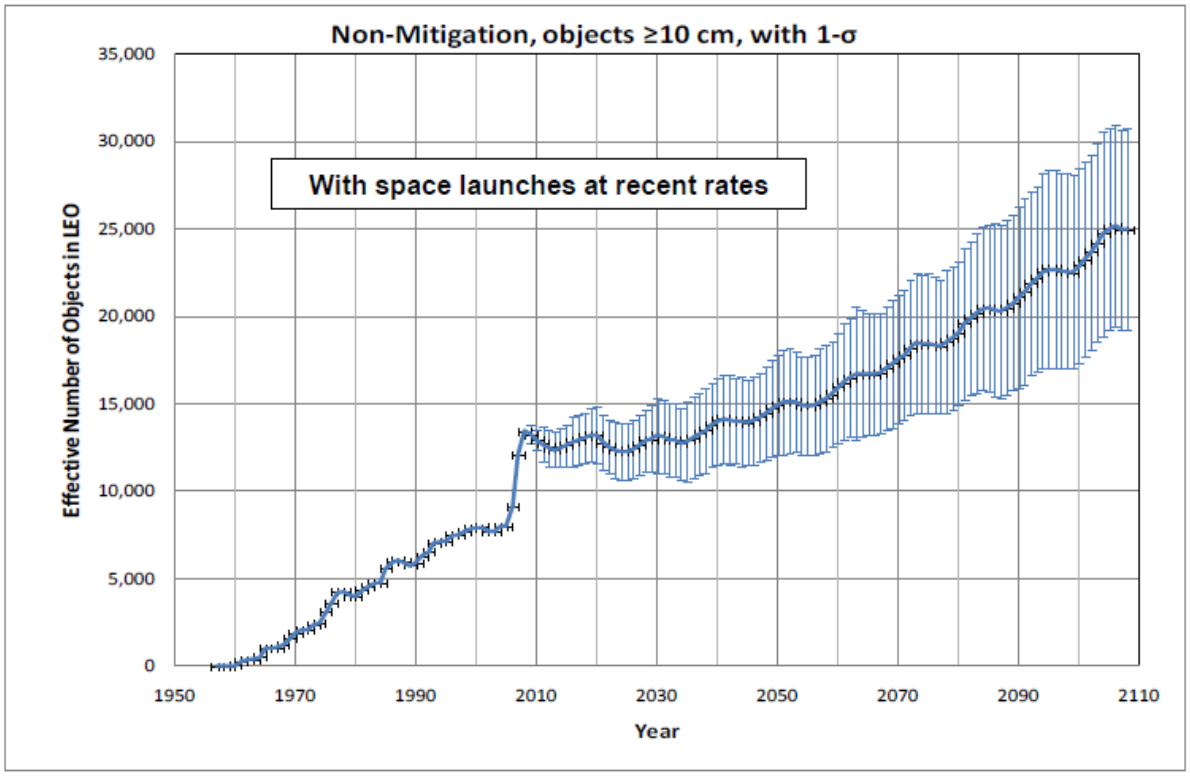

Figure 13: The effect of Chinese ASAT test in 2007 and the collision of Iridium 33 and Cosmos 2251 in picture. [52]

3.3 Mitigation techniques:

3.3.1 Prevention:

'Prevention is better than cure'- says it all. In order to reduce the future chances of fragmentation, preventive methods include some mission specific guidelines and regulations.one method is the Passivation Technique. This simply suggests the de-orbiting or disposal of a satellite at the end of its life. All satellites carry residual fuel on board the satellite. The propellant is used during the entire mission lifetime of the satellite and one final thrust is produced by burning the rest of the propellant in order to dispose the satellite. For Leo satellites, this is done by reducing the perigee altitude and bringing the satellite in to the lower altitude. The Earth's atmosphere does the rest by burning it. In case of GEO satellites, the mission lifetime is quite higher, due to the invention of Electric propulsions, some of them now can enjoy a lifetime up to 15-18 years. And then one final burn takes it to the 'Graveyard orbit', some 300km above GEO, which makes both the GEO spot free for the next satellite and avoidance to some further collisions or fragmentations events.

All the space fairing nations are contributors to orbital debris due to their space activities, and the risk is to all. Individual policies are taken to mitigate and control debris situations, like NASA, DOD, SSN, ESA etc.

Organizations like International Astronomical Congress (IAC), United Nations (UN), European Space Agency (ESA), Japan Aerospace Agency (JAXA) and the Inter – Agency Debris coordination Committee (IDAC) making combined efforts to make different space activist nations help and understand the situation and come up with a preventive solution. As a result, Actions like Passivation, Disposal at EOL[14] and space weapon bans are in practice [15].

3.3.2 Protection:

Spacecraft outer surface if often contains a shielded layer to protect the impacts from MMOD and manmade debris in the orbit. The early days shielding method was based on the usage of Monolithic Aluminum layers on the outer surface. Even though this was good enough to protect the Geo satellites, for LEO satellites and the increasing number of LEO space chunks this is considered as 'Old fashioned'. In LEO, the typical velocity of debris is about 11km/s. this is

[14] End of life of a Particular satellite mission.

not the end, this might go up to 20km/s as the penetrable MMOD travels at that speed near LEO.

A relative smarter shielding technique is the '*Whipple Shielding*'; which has a *Bumper* made of Aluminum sheet at distance from the rear wall with a *sandoff* in between the two walls. As the projectile impacts on the Bumper wall. Both the projectile and wall debris are expanded inside the *sandoff* which results the momentum of the impactor being distributed over a wider area of the rear wall. The rear wall must be thick enough to withstand the fragments and blasts from the cloud materials. Over the recent years, improved shielding technique has been introduced along with the '*Whipple Shielding*'. Usage of Nextel™ ceramic fabric and Kevlar™ high strength fabric in terms of a blanket that incorporates the shielding outside the bumper wall and inner pressure wall. This has significantly increase the protecting efficiency and decreased the shielding mass at the same time. [16]

3.3.3 Avoidance:

Collision avoidance has become a routine and essential part of spacecraft mission in LEO satellites these days. Evidences have been found responsible for delays in launch and mission performance. In the early 2nd and 3rd quarter of this year ISS has to go through two collision avoidance maneuvers in space. The first PDAM[15] was on 23rd April to avoid some close approaches of catalogued debris originated from the METEOR 2-5 satellites. The second maneuvere took place on 8th June this year to avoid a close conjunction with a fourth stage rocket body that was used to launch STPsat -3 and 28 cubesats. 'A shelter-in- place' was performed on the 16th July, 2015, due to insufficient time to perform a PDAM. The ISS crews took shelter in the Soyuz module for safe return to Earth in case there was a breach in the ISS due to the METEOR 2-5 fragments conjunction with ISS. [17]

[15] Planned Debris Avoidance Manuevere

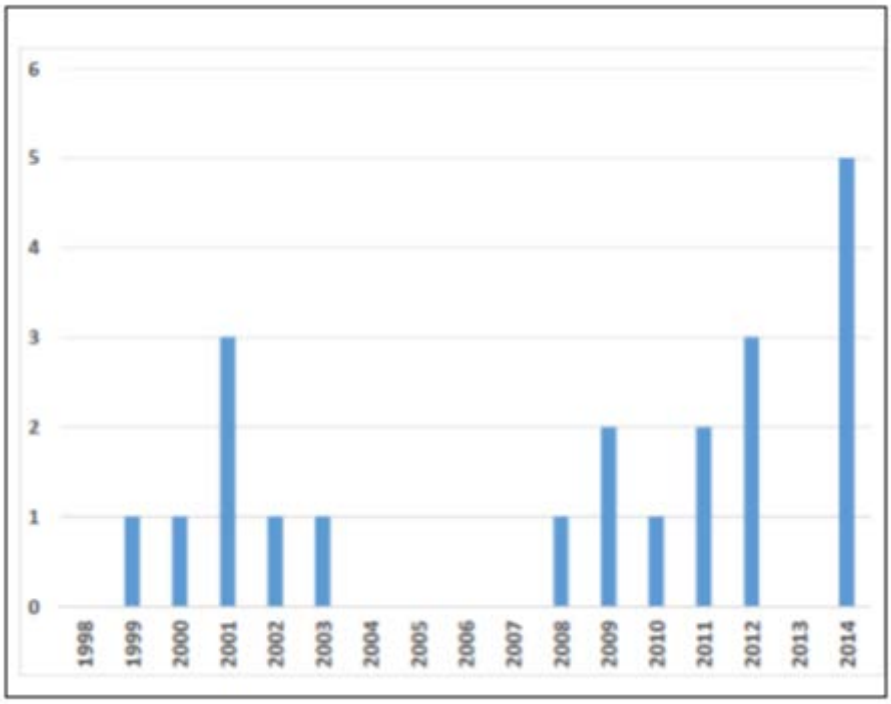

Figure 14: ISS planned PDAM since the first module launch in 1998 [18].

3.3.4 Passive removal:

Passive removal of Debris do not require any controlled interactions. This makes it easier since there is no need of attitude control or thruster burns. The uncontrolled interaction means only one thing: slowing down the Debris and let them fall in a lower orbit and the Drag force from the upper Earth Atmosphere does the rest. Decaying the orbit this way has the advantages over all sizes of Debris. Even though passive method is an effective way to mitigate space debris, this is rather quite slow process and today the orbital debris has reached to a certain population density that self-removal or causing the re-entry by slowing the debris is not the most efficient way of doing it. One passive removal method is Misting; a well-placed spray of mist creates some sort of clouds that induces a drag force. This Drag force then causes the objects passing through it to slow down and orbit decays [19]. Another effective passive removal technique is to put a Slab of Polyimide Foam in a targeted orbit. The space chunks in that targeted orbit when passing through the Foam Slab slow down and their orbit starts to decay [20]. Several techniques of passive removal of debris of the similar types do exist today, each of them uses different medium or structure to interact with the aim to cause the orbit decay. One major drawback of passive removal technique is: it can make no difference between an operational satellite and a debris. [21]

3.3.5 Active removal:

Active debris removal requires some sort of controlled interaction with a target body in the orbit; hence this method works well only with debris those are large enough to apply the removal method. Several types of Laser Impingement techniques have been already proposed to remove debris actively. The laser beam operated either from the Ground or from the Space create a surface pressure on a leading edge of Debris. This causes the debris slow down and in consequence orbit decay [22] [23]. Another proposal was to use Ion beams instead Laser beams [24]. The above methods are quite useful in a sense that, they do not require orbit transfers which is costly, rather they can be operated from distance. Again, more works are needed to carry on for the feasibility. It is also not clear whether longer exposure of beams will lead to material fragmentation; this will make the whole process even more complicated.

3.4 Worldwide Space Debris Mitigation Policies:

3.4.1 United States:

All U.S. government requirements and commercial regulations for orbital debris mitigation are derived from the U.S. Government Orbital Debris Mitigation Standard Practices which are cited in U.S. National Space Policy [52]

The standard practices according to USG Orbital Debris mitigation policies has the following standard practices:

1. Minimizing the mission related debris and limit LEO space debris lifetime to a maximum of 25 years.
2. To use designs and procedures in order to avoid during mission operation and post disposal breakup events.
3. Protection against collision events with small debris and avoid larger debris for a collisional event.
4. Limiting a post mission lifetime of 25 years in LEO to avoid casual reentry to upper Earth atmosphere. In GEO a post mission manuevere needs to be performed 300km above GEO.

3.4.2 Inter-Agency Space Debris Coordination Committee (IDAC):

All the Space Agencies together with twelve leading space agencies in the world including Canada, China, France, Germany, Italy, India, Japan, Russia, Ukraine, United Kingdom and United States as well as ESA have developed the First Consensus of orbital debris mitigation guidelines in October 2002; which was slightly revised in 2007 [52]

3.4.3 United Nations:

In February 2007, STSC Member States adopted space debris mitigation guidelines and also adopted the full COPUOS in June 2007. The full General assembly was adopted in late 2007.

3.4.3 National policies:

Who	When	What
Japan	March,1996	Space Debris Mitigation Standard (NASDA-STD-18A)
France	April, 1999	CNES Space Debris –Safety Requirements (MPM-50-00-12)
Russia	July, 2000	General Requirements for Mitigation of Space Debris Population (Branch Standard)
China	July, 2005	Requirements for Space Debris Mitigation (QJ 3221 –2005)
ESA	2006	European Code of Conduct for Space Debris Mitigation

Table 3: Mitigation policies taken by different space fairing nation.

3.5 Debris Detection Methods:

3.5.1 Radar- Based Earth Observation:

Many Radar Observatories worldwide including SSN use Radar-based debris detection technique to catalogue them. The main drawback of using this method is the limitation of required power to get a return signal back from LEO. Object size determination is limited with the radar resolution cells size versus the size of the target object in orbit. The target body has to be at least ten times larger in size than the radar cell resolution size [25] [26]. The German Tracking and Imaging Radar System has been sensing the space debris in LEO. The TIRA is able to produce two-dimensional imaging of the debris by using the Inverse Synthetic Aperture Radar (ISAR) along with Radar Range profiles [25] [26]. A series of Radar Images leads to the analysis of the rotation rate and rotation direction of an in orbit objects. Some authors have presented an Algorithm to generate high-resolution 3D images from ISAR images [27]. An alternative method is Single Range Doppler Inferometry (SRDI); that allows imaging of objects

smaller that the range resolution size of the Radar. This method is used with the aim of solving sparse signal reconstruction problem which is then able to image objects in the range of 1-10cm in diameter [28] [29].

3.5.2 Optical Observations:

Optical observation is the most studied and effective effort so far to categorize and detect orbital debris. The Air Force Maui Optical and Supercomputing (AMOS) detachment on Maui has three systems those can be used for optical and thermal imaging for debris, [30] [31] [32]. The 3.67 m telescope at AMOS, which is an Advanced Electro Optical System telescope contains an adaptive system to image LEO debris, anomalous events and breakup events, [30]. The Liquid Mirror Telescope (LMT) operated by NASA is able to detect debris down to 3cm in diameter. Another telescope operated by NASA is the Charged Couple Device Debris Telescope to track the debris in GEO.

On behalf of ESA, The Astronomical Institute of the University of Bern (AIUB), operates a 1m telescope to analyze the Higher Area-to-Mass Ratio (HAMR) in GEO and GTO region. Optical observations, through the analysis of light curves, from the AIUB telescope are used for the initial orbit determination process and then determination of orbits for HAMR objects. A small debris catalogue build up effort was taken via photometry and light curves from the 1m telescope data for HAMR shape and attitude state for GEO. [33] [34]. Ground based Electro-Optical Deep Space Surveillance (GEODSS) telescope is used to determine the albedo of debris [35]. In order to convert the visual brightness to physical size, the albedo of an object must be determined. The findings from Infrared and optical measurements suggests that the debris have a lower albedo than their origin (satellites), since they go through darkening effects after breakup and fragmentation. Simulated photometric data is used to determine the materials properties of the debris. Once the material is known, the corresponding albedo can be determined [36].

Space-based telescopes those were launched into LEO, GEO and GTO to pursue initial orbit determination, surveillance and GEO objects characterization, originate from the concepts covered in [37] [38]. A 15cm aperture telescope was proposed in [37] for observing uncontrolled GEO objects; aiming to track down objects to 1cm in diameter.

3.5.3 Thermal and IR methods:

Advanced Electro Optical System (AEOS) telescope at AMOS has been in use to observe the HAMR in GEO [39] [40]. AEOS consists Broadband Spectrograph System (BASS) sensor which is a mid-wave infrared device, sensitive in the range 300-1300 mm band wavelength of the spectrum. Observation data which includes thermal and material properties affect the solar radiation pressure incident upon the HMAR objects and helps modeling near accurate orbits [39]. Sometimes the IR measurements are coupled with CCD measurements. Together it allows the characterization of space debris through temperature determination, materials and orientation dynamics [40].

In 1983, the Infrared Astronomical Satellite (IRAS) was launched with a multi-band infrared sensor onboard the satellite to perform an all-sky survey. The satellite was placed in an 800km Low Earth, Polar sun synchronous orbit. The sensor could operate in four different wave bands centered at 12, 25, 60 and 100 micrometer respectively. The sensor data is useful for determining temperature, absorptivity and physical size of the satellites [41].

Thermal imaging techniques of space debris based on both space and ground based methods using radiometry data are presented in [42] and [43]. The first author presents the analytical modelling for the thermal imaging of debris while the second author presents a method to analyze the uncertainty in the parameter data.

Characterization techniques for small satellites and space debris are presented by some researchers using optical and infrared observation [44]. Where the characterization techniques include determination of semi major axis, size, mass and albedo. The methods those were proposed for characterization involved photometry, radiometry and spectroscopy analysis.

3.5.4 In –Situ measurements and retrieved surfaces:

The main limitation of Ground based radar and optical instruments is the Earth’s Atmospheric attenuation for both in visible and radio frequency. Another important fact is the reflected energy dispersion by a radar is inversely proportional to the fourth order of the slant range; for a telescope, it is inversely proportional to the square of the slant range. [45].

Many of the limitations can be overcome by simply placing the instruments in higher Earth atmosphere or placing them directly in to the orbit. Since 1960, many optical instruments in the visible, Infra-Red. X ray or Gama ray frequencies are in operation in orbit. Some of this instruments have also produced amazing space debris data just as a byproduct of the primary mission objective. The Infra-Red Astronomical satellite (IRAS) was launched in 1983 with the primary mission objective to scan the celestial sphere in the IR band; about 10 years later, a total of almost 200,000 tracks of non-celestial objects were imaged. [45].

Another well-known Optical sensor in space is Hubble Space Telescope (HST) which was launched in 1990. During the extra vehicular servicing of HST and a solar panel retrieval occasion, many small particle impact were detected in the millimeter range diameter. Long Duration Exposure Facility (LDEF) was another important source of in-situ meteorites and space debris detection. Launched in 1984, it had a total of 130 m^2 impact area. After 5.7 years of space exposure, the post flight analysis revealed almost 30,000 impacts in which almost 5000 were visible with the naked eyes. [45].

In July 1992, the European Retrievable Career (EURECA) spacecraft was launched in space in order to study the impacts of debris. EURECA had 140 m^2 impact surface to collect data, in which 96 m^2 contained in the front and back side of the solar arrays. After the post flight inspection, traces of ~2,000 impacts were found [45].

Several other space returned hardware were analyzed for impact features. Some of them are: Japanese Space Flyer Unit (SFU), Russian Salyut Flights 1 to 7 and the Mir mission. The returned hardware gives us the answer to the questions like: the origin of the impactor (whether man-made or meteoroid), size of the impactors as well as impactor velocity and impact direction. But what is unanswered is the epoch at which the impact occurred and the orbital position [45].

Technosat, a German satellite from TU Berlin and German Aerospace Agency (DLR) has also built and awaiting for the launch a Space Debris Detector (SOLID) on board a nanosatellite for In-Situ experiments in the LEO. In the later sections in this thesis, the implementation and test of the SOLID will be explained in details.

4. TechnoSat and SOLID :

TechnoSat is a German Nano satellite Mission being developed mainly by TU Berlin (Technical University Berlin) with the association with DLR (German Aerospace Center). Weighing about 20Kg, and a dimension of 300 x 450 x 450 mm, TechnoSat is aimed to perform the On Orbit Demonstration of New Nanosatellite Technologies for its One year lifetime. Thus the primary mission Objective of TechnoSat is to demonstrate the on Orbit verification of the Novel Nanosatellite Technology [46]. Among the new technologies, the Solar Generated Impact Detector (SOLID) is the prime focus for this thesis work.

As a secondary mission objective, comes the development and demonstration of TUbiX20 Nanosatellite BUS onboard the Octagonal structural shaped TechnoSat [47].

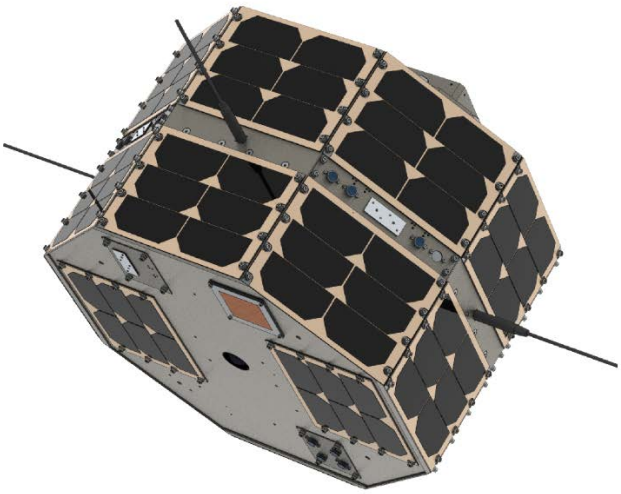

Figure 15: Schematic Diagram of TechnoSat [46]

4.1 Technologies On Board Technosat :

TechnoSat carries several payloads to demonstrate some new technologies for Nanosatellites. The primary selection of payloads [46] - [49] contains the following:

- Camera
- Fluiddynamic Actuator
- S-Band Transmitter HISPICO
- Laser-Retroreflectors
- Solar Generator Impact Detector (SOLID)
- Star Tracker STELLA
- Rection Wheel System

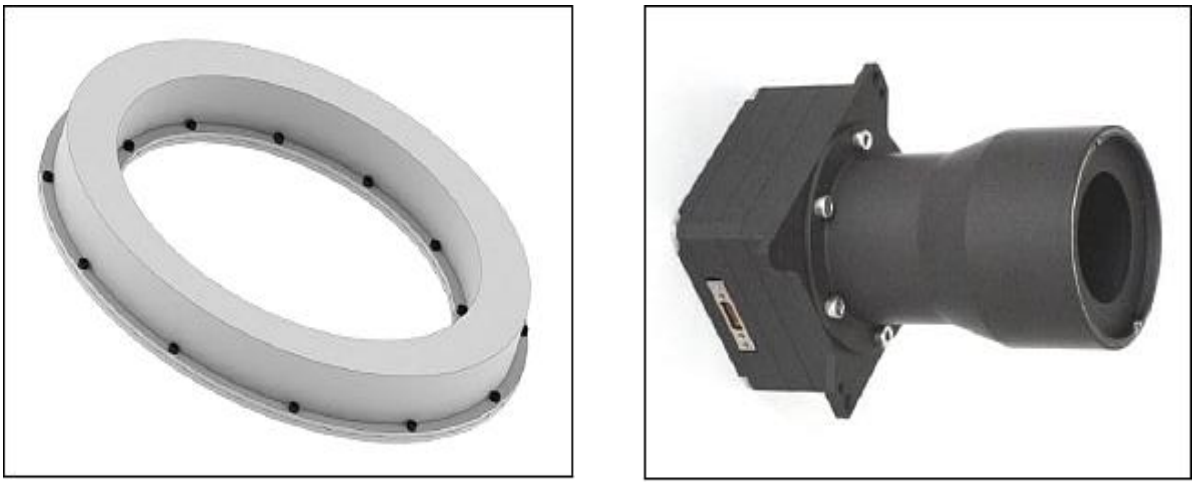

Figure 16: (a) Fluid dynamic Actuator. (b) Miniature Star tracker STELLA [46].

4.2. SOLID Electronics:

The Solar Generated Impact Detector (SOLID) payload is mounted on the solar panel surface of the octagonal Shaped TechnoSat. In total there are eight surface panels, so the SOLID hardware. Each panel of SOLID hardware consists 3 PCA9505 Multiplexers (MUXs) / De multiplexers (DEMUXs) and an I2C switch PCA 9546A. The I2C switch is connected to the STM32 Discovery microcontroller via I2c BUS interface. The switch able to select and deselect the different multiplexers. The pins in the multiplexers are configures as OUTPUT or INPUT pins. All the pins are laid out in a mesh or Matrix format and gives the Cartesian positions. Whenever there is an impact on the surface panel, the corresponding position can be located and mapped by telemetry data in Ground station. A Graphical User Interface (GUI) is able to map the impact locations and the corresponding surface panel. Thus SOLID will collect one year mission data and will be able to map the number of impacts in the specific mission orbit. Since, SOLID is not a retrievable Space Hardware, a GUI will be the best and feasible option in order to demonstrate and visualize the in orbit impacts on Ground. A brief but necessary description of the SOLID hardware will be described below before the interfacing and accessing of the hardware is implemented.

Figure 17: SOLID- TechnoSat block Diagram.

4.2.1. MUX/ DEMUX

A Digital Multiplexer or MUX is an electronic circuit which is able to switch or control the several input data to pass through one output data. The simplest MUX can be as simple in form as a rotary switch; which can switch between several different inputs to one output based on the selected position of the switch as an input. For faster switching applications, the multiplexer is needed to be controlled electronically, rather than mechanically. Whereas Analog Multiplexers are controlled by relays or resistors, digital multiplexer switches are controlled by digital logic gates to switch one of the inputs through a single output [50].

The reasonable and most common application for a MUX would be a Parallel to Serial digital data converter. Where the input data are in Binary format and the output is a serial data stream of the transferred data. For example a 1-of-8 MUX would convert an 8 bit serial data from an 8 bit parallel data input. Data select lines are included in the MUX circuit to select the input data lines. An N select lines would be able to select a total of 2^N input lines of a MUX.

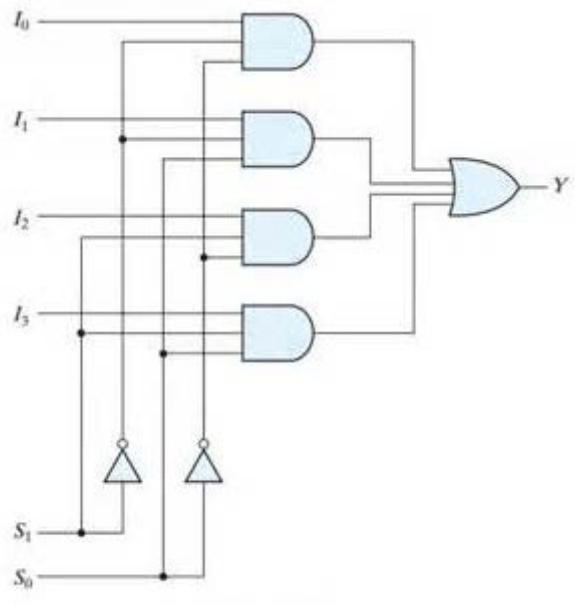

Figure 18: A 4-to-1 MUX construction with logic gates.

Digital De-multiplexers or DEMUXs work the opposite way that of the MUXs. So, a DEMUX is a data distributor rather than selector. The serial Data input is distributed over one of several Output lines. In this regard, the Basic functionality of a DEMUX circuit is Serial to Parallel Data conversion. Like MUXs, the DEMUXs also need to be controlled by electronic logic gates

for high speed and faster data transmission. Transmission of Data over parallel lines are much faster compared to serial data transmission. But this requires more dedicated and parallel data transmission lines; which is expensive. So, in most cases parallel data are converted into serial format before long distance transmission and then again a DEMUX is used on the receiver end if necessary.

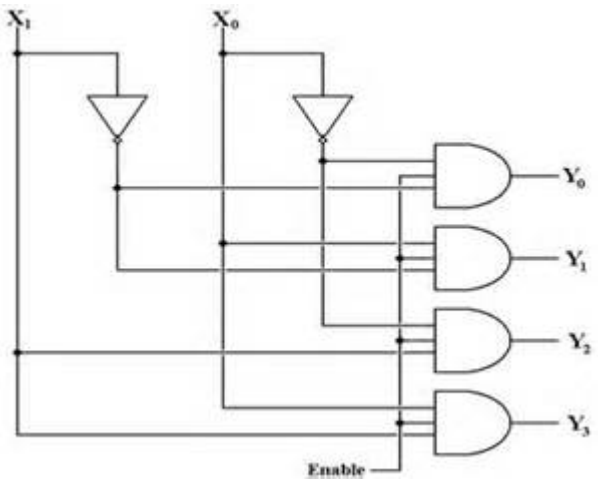

Figure 19: A 2-to-4 DEMUX circuit.

4.2.2. PCA 9505 I/O Expander:

It provides 40-bit parallel Input/output (I/O) port expansion for I2C bus expansion. The 40 ports are organized in a total of 5 banks of 8 I/Os each. All the 40 ports can be configured as either input or output ports. With the aid of +5V power supply, the outputs are capable of sourcing 10mA and sinking 15mA current. Even though another version of PCA 9505 is available as PCA 9506, it does not include any internal pull up resistors to reduce the power consumption. PCA 9505 has built in 100kΩ internal pull up resistor, so it reduces the power consumption in all the I/Os. PCA 9505 can be operated either in 100 kHz (Standard Mode) or 400 kHz (Fast Mode), which is compatible with I2C serial Bus interface. [Product Datasheet, NXP Semiconductors]

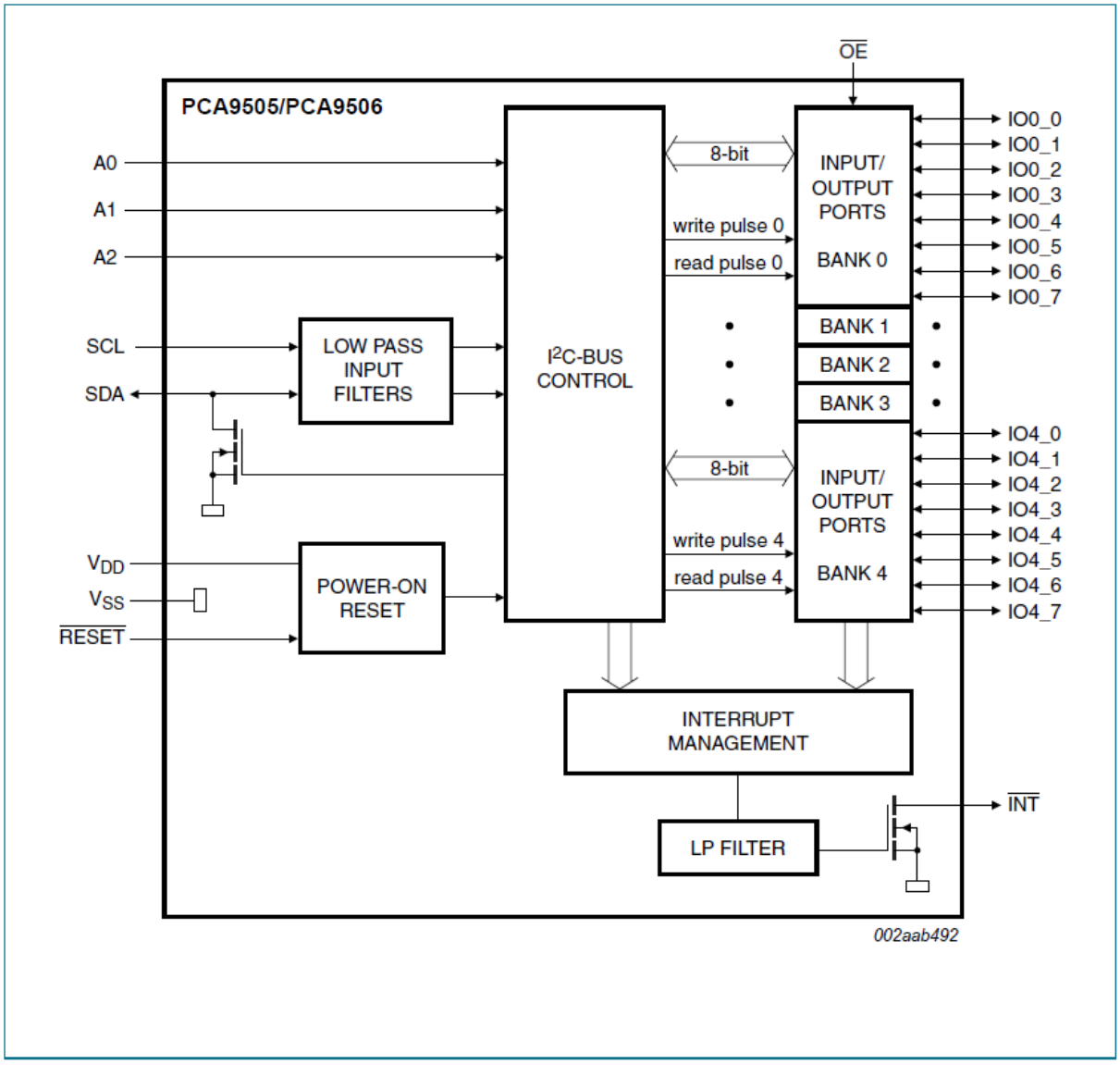

Figure 20: PCA 9505 /PCA 9506 Block Diagram.

4.2.2.1. PCA 9505 Device Address:

The Bus Master sends the Slave Address after the START bit to access the device and perform the operation it wants to (Read or Write). PCA 9505 has three slave or device address pins (A0, A1 and A2). In order to reduce the power consumption, no pull up resistors are connected internally. The last bit of the slave address byte indicates the desired operation to be performed. 1 is Read and 0 selects Write operation.

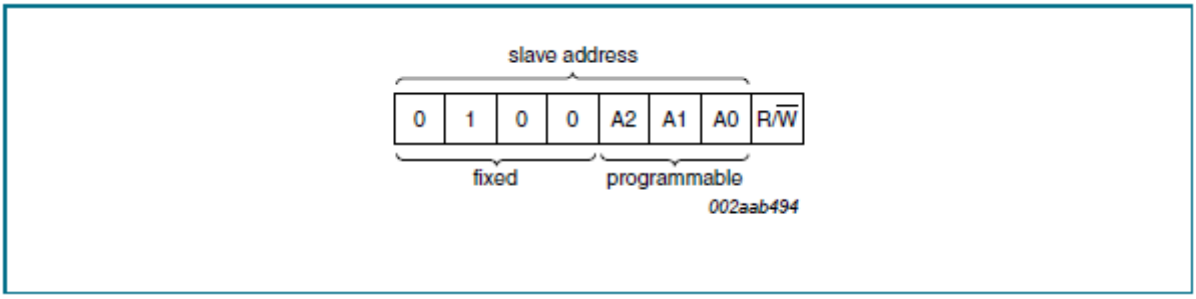

Figure 21: Data Byte for Device Address

4.2.2.2. PCA 9505 Command Register:

After the successful acknowledgement of slave address and Read/Write byte, the Bus Master sends one byte data to PCA 9505, the data byte is then stored in the Command Register. The last 6 bits (D5 to D0) is used to determine the type of the registers. When the AI (Auto Increment) bit is set to 1; it allows bits D2 to D0 to change and thus giving the user a sequential access (read or write) to all the register banks. But after 5 bytes of Data is written with AI = 1, the next Data byte will be overwritten.

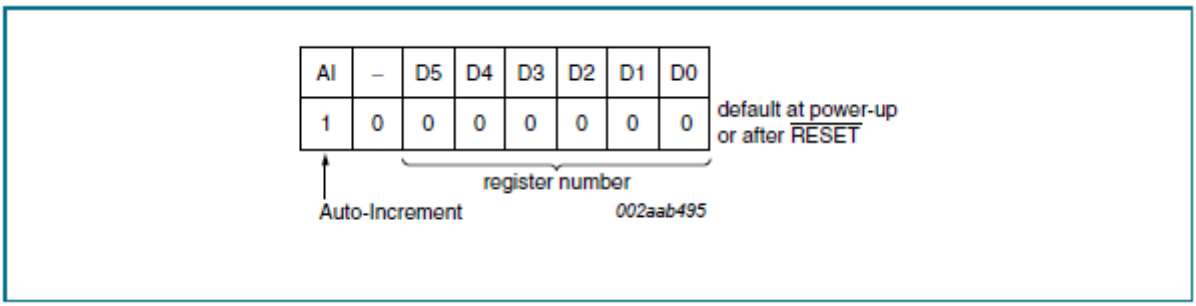

Figure 22: Data Byte stored in Command Register.

Selecting AI=0 will not give the sequential access to all register banks. In this case, the same register bank will be read and written repeatedly. For all cases, the Reserved Registers are skipped by default.

Command Register (CM)	Type of CM	Total Numbers of CM
IP	Input Port Register	5
OP	Output Port Register	5
IP	Inverse Polarity Register	5

IOC	I/O configuration Register	5
MSK	Mask Interrupt Register	5

Table 4: Different Register Blocks for PCA 9505.

4.2.2.3. Input Port Registers (IP0 – IP4):

These are Read Only Registers; they reflect the incoming logic levels of the Port Pins, irrespective of the fact that the Input Port register has been defined as Input or Output. Also, changing the bit value in the Polarity Inversion Register (PI), does not put any effect on Writing to these input Port Registers.

Address	Register	Bit	Symbol	Access	Value	Description
00h	IP0	7 to 0	I0[7:0]	R	XXXX XXXX*	Input Port register bank 0
01h	IP1	7 to 0	I1[7:0]	R	XXXX XXXX*	Input Port register bank 1
02h	IP2	7 to 0	I2[7:0]	R	XXXX XXXX*	Input Port register bank 2
03h	IP3	7 to 0	I3[7:0]	R	XXXX XXXX*	Input Port register bank 3
04h	IP4	7 to 0	I4[7:0]	R	XXXX XXXX*	Input Port register bank 4

Figure 23: corresponding addresses of IP Registers.

4.2.2.4. Output Port Registers (OP0- OP4):

These registers reflects the outgoing logic levels of the pins those are defined as Output by the IO configuration register. The reading from these registers does not represent the actual pin values, rather gives the flip flop values which is controlling the output selection.

Address	Register	Bit	Symbol	Access	Value	Description
08h	OP0	7 to 0	O0[7:0]	R/W	0000 0000*	Output Port register bank 0
09h	OP1	7 to 0	O1[7:0]	R/W	0000 0000*	Output Port register bank 1
0Ah	OP2	7 to 0	O2[7:0]	R/W	0000 0000*	Output Port register bank 2
0Bh	OP3	7 to 0	O3[7:0]	R/W	0000 0000*	Output Port register bank 3
0Ch	OP4	7 to 0	O4[7:0]	R/W	0000 0000*	Output Port register bank 4

Figure 24: corresponding addresses of OP Registers.

4.2.2.5. I/O Configuration Port Registers (IOC0- IOC4):

These Registers configure the I/O port registers either as input or output.

If IOC_x[y]= [0] then the corresponding port pin is in Output state.

If IOC_x[y]= [0] then the corresponding port pin is in Output state. Where, x corresponds to the bank number (0-4) and y corresponds to the pin number (0-7).

Address	Register	Bit	Symbol	Access	Value	Description
18h	IOC0	7 to 0	C0[7:0]	R/W	1111 1111*	I/O Configuration register bank 0
19h	IOC1	7 to 0	C1[7:0]	R/W	1111 1111*	I/O Configuration register bank 1
1Ah	IOC2	7 to 0	C2[7:0]	R/W	1111 1111*	I/O Configuration register bank 2
1Bh	IOC3	7 to 0	C3[7:0]	R/W	1111 1111*	I/O Configuration register bank 3
1Ch	IOC4	7 to 0	C4[7:0]	R/W	1111 1111*	I/O Configuration register bank 4

Figure 25: corresponding addresses of IOC Registers.

4.2.2.6. I2C Bus transfer:

I2C is a bi-directional and two line communication between two ICs, where the two lines are SDA (Serial Data Line) and SCL (Serial Clock Line). In order to initiate communication between devices, the both lines should be connected to positive power supplies. One Data bit is transmitted during each clock pulse. SDA should remain stable during HIGH clock pulse while transmitting Data to avoid interruption. The availability of Bus line depends on both SDA and SCL in HIGH state. A HIGH –LOW combination denotes transmit of START bit and LOW-HIGH is the state for STOP bit. In both cases the clock pulse remains HIGH. Some schematics are presented to explain the different operations on I2C BUS.

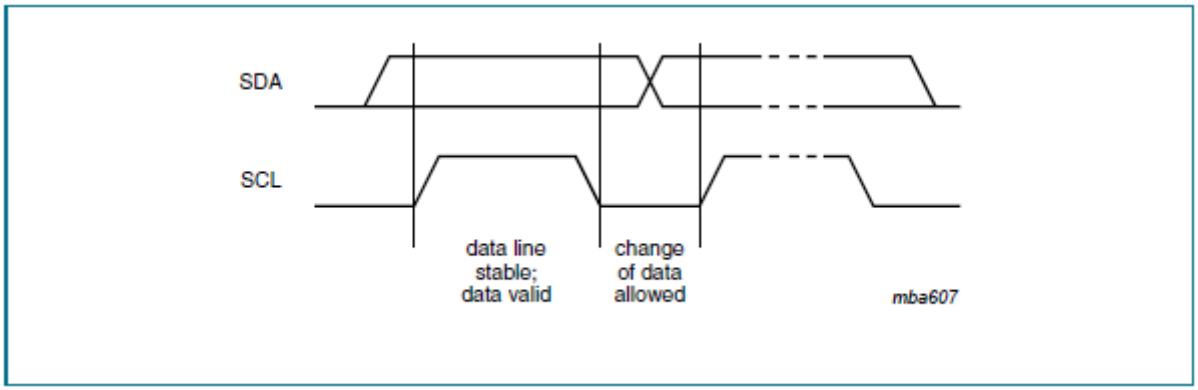

Figure26: Bit Transfer in I2C Bus.

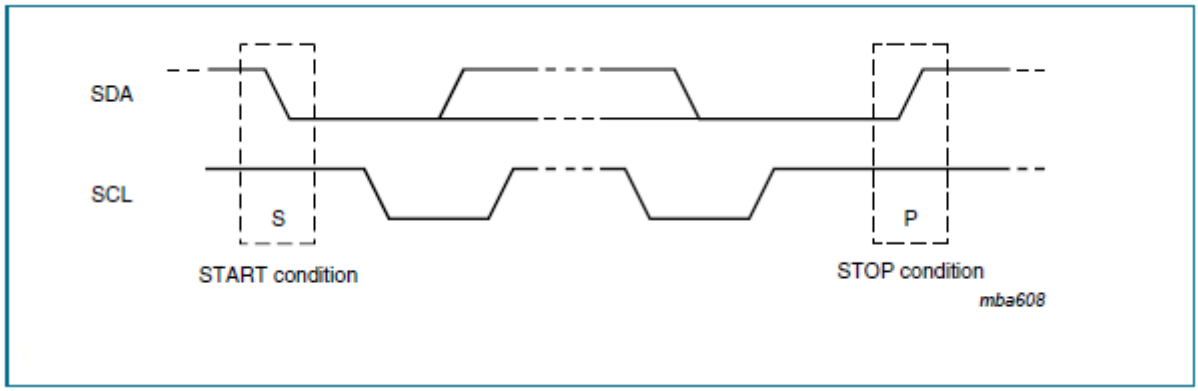

Figure 27: START and STOP condition.

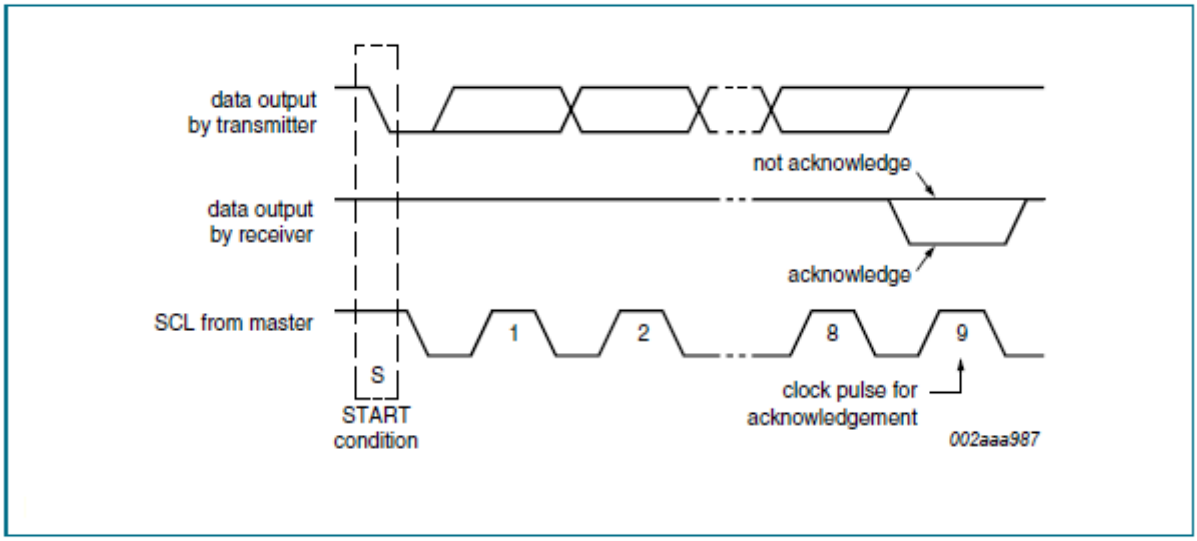

Figure 28: Acknowledgement on I2C Bus.

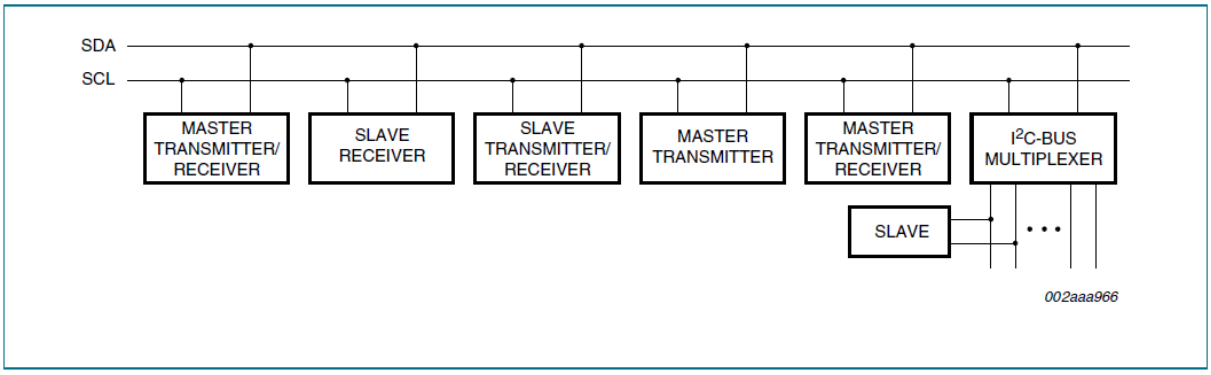

Figure 29: system configuration in I2C bus as Master and Slave.

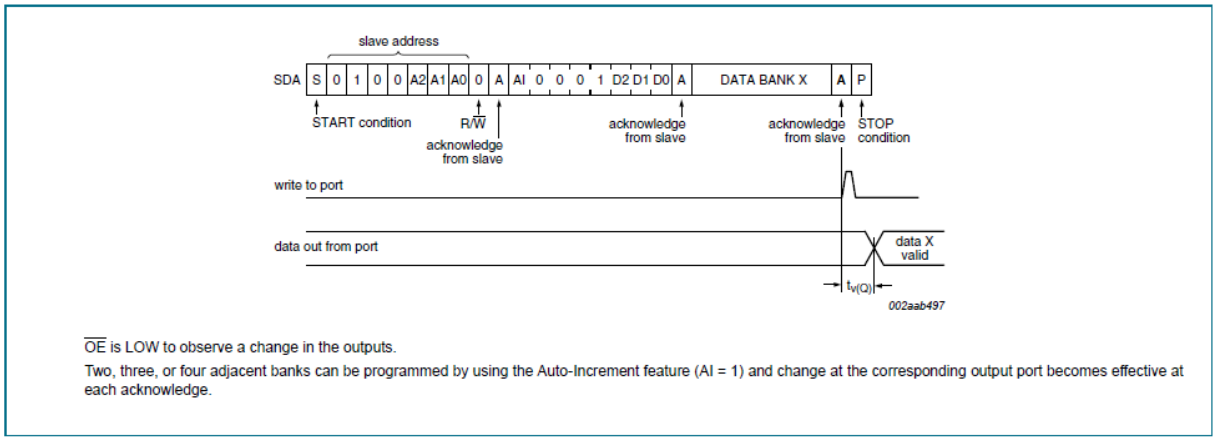

$\overline{OE}$ is LOW to observe a change in the outputs.

Two, three, or four adjacent banks can be programmed by using the Auto-Increment feature (AI = 1) and change at the corresponding output port becomes effective at each acknowledge.

Figure 30: Write to a specific output port.

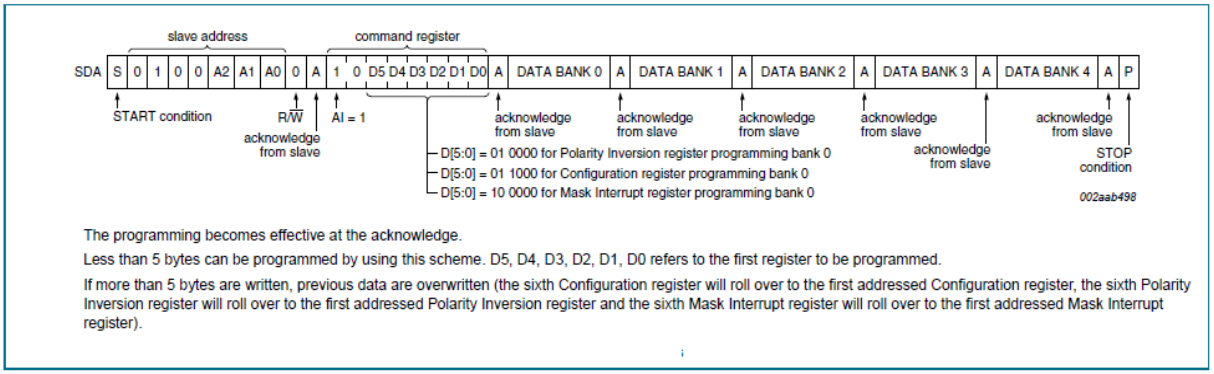

The programming becomes effective at the acknowledge.

Less than 5 bytes can be programmed by using this scheme. D5, D4, D3, D2, D1, D0 refers to the first register to be programmed.

If more than 5 bytes are written, previous data are overwritten (the sixth Configuration register will roll over to the first addressed Configuration register, the sixth Polarity Inversion register will roll over to the first addressed Polarity Inversion register and the sixth Mask Interrupt register will roll over to the first addressed Mask Interrupt register).

Figure 31: Write to the IOC or PI or MSK registers.

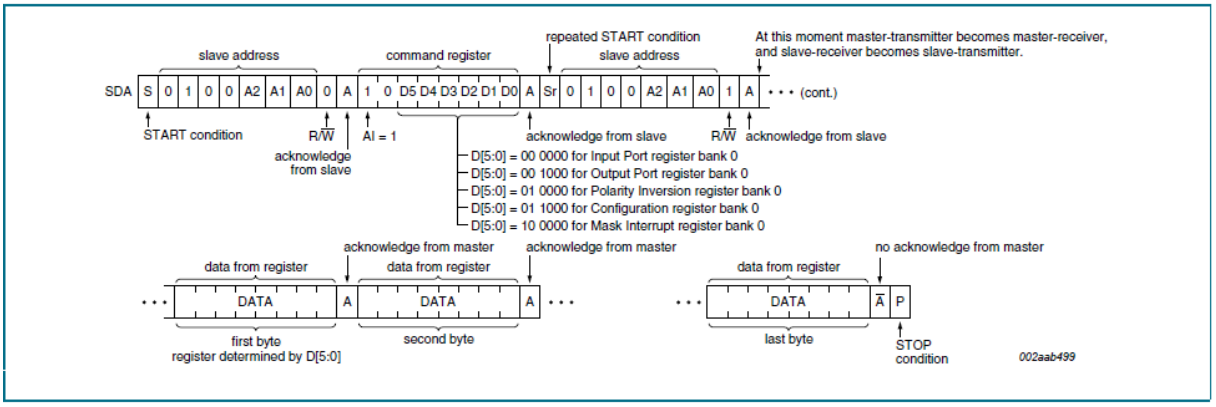

Figure 32: Read from IP, OP, IOC, PI and MSK registers.

4.2.3. PCA 9546A I2C- Bus Switch:

PCA 9546A is a 1-of-4 bidirectional translating switch which is controlled by I2C bus. The switch has 3 bit address pins which allows up to eight devices to add on the I2C bus. Any SDx/SCx or a combinations of Channels can be selected via I2C bus. The operating Voltage of

the switch is between 3.3V and 5.5V with 0Hz to 400 kHz clock frequency and all I/O pins are 5V tolerant. The switch can limit and translate voltage levels between 1.8V, 2.5V, 3.3V and 5V. In the SOLID hardware design, the switch uses 3 channels to control and translate 3 PCA 9505 IO Expanders, one at a time or a combination of them.

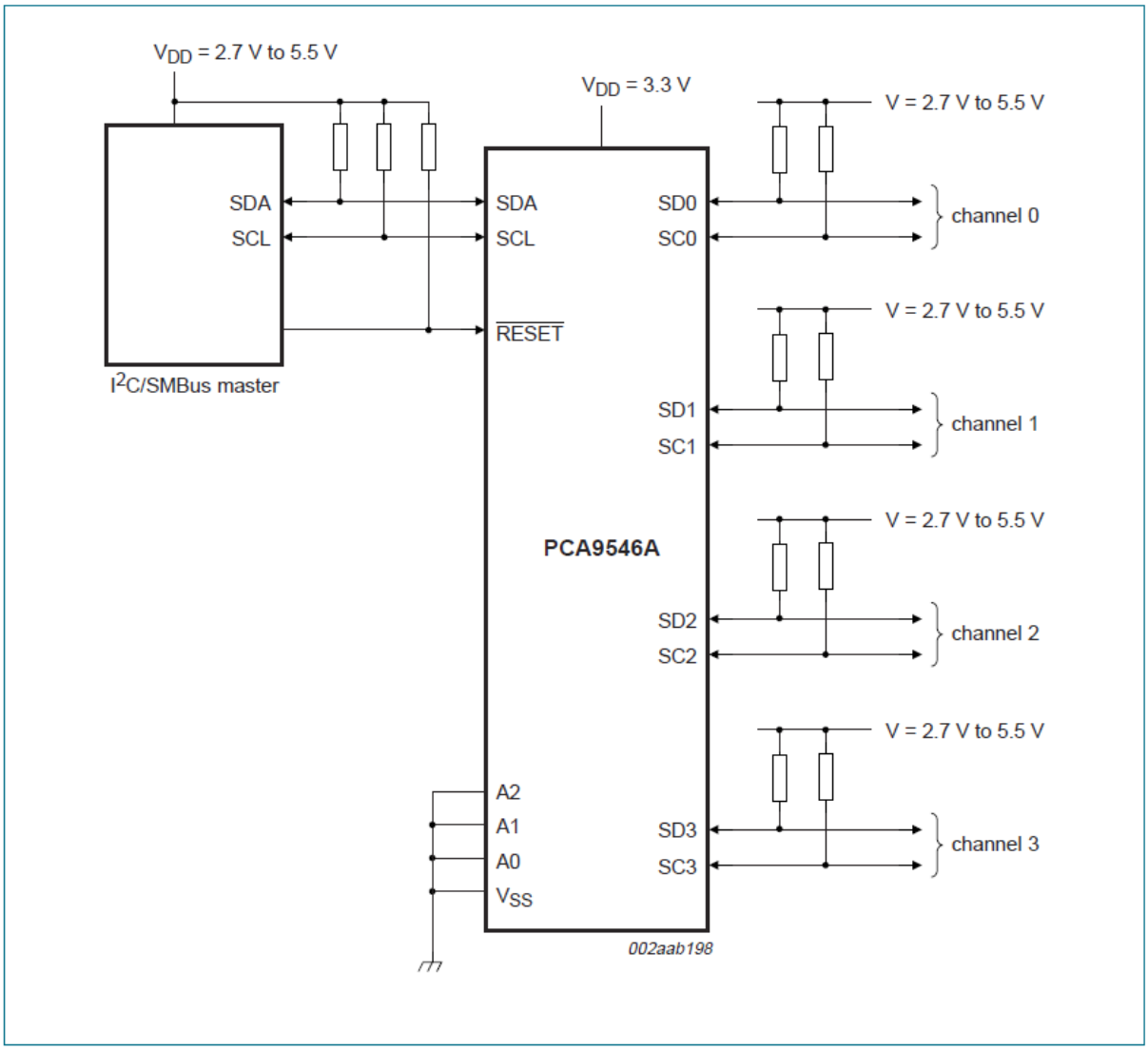

Figure 33: Application Diagram of PCA 9546A I2C Bus Switch.

4.2.3.1. Device Address:

Following the START bit, the Bus master has to produce the slave address it wants to access. The last four bits of the address byte can be programmed in order to access an IO Expander. Since there are three IO Expanders in each panel of SOLID hardware, one channel address is unused. The least significant bit of the Address byte is set to 1 for a Read Operations and set to 0 for a Write operation.

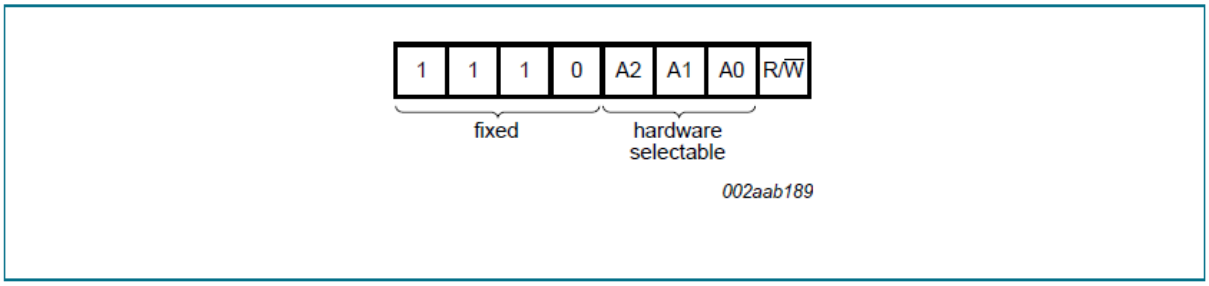

Figure 34: PCA 9546A Bus Address configuration.

4.2.3.2. Control Register:

Following a successful AKN, the bus master sends a byte to save in the control register. In case of multiple bytes, PCA 9546A saves the last byte. The control register is read and Data Byte is written in the register using I2C bus.

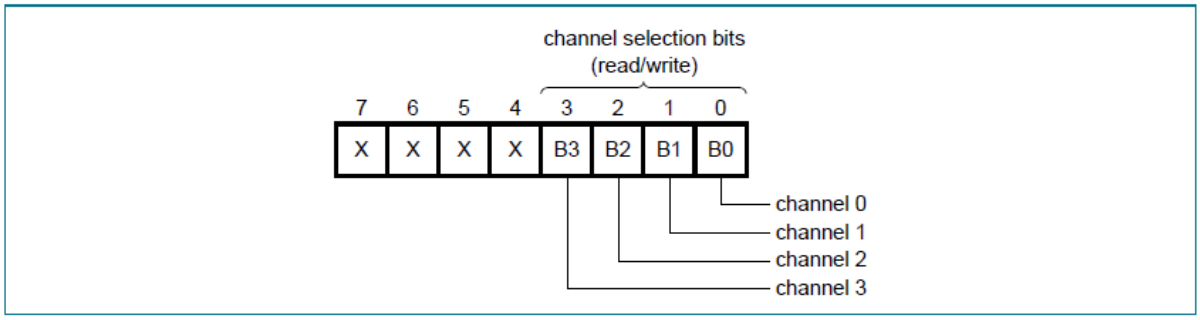

Figure 35: PCA 9546A channel selection.

4.2.3.3. Definition of Control Register:

One or several channel can be selected after the PCA 9546A switch has already been addressed. The last four bits determine which channel is going to be enabled, so a combination of channels

D7	D6	D5	D4	B3	B2	B1	B0	Command
X	X	X	X	X	X	X	0	channel 0 disabled
							1	channel 0 enabled
X	X	X	X	X	X	0	X	channel 1 disabled
						1		channel 1 enabled
X	X	X	X	X	0	X	X	channel 2 disabled
					1			channel 2 enabled
X	X	X	X	0	X	X	X	channel 3 disabled
				1				channel 3 enabled
0	0	0	0	0	0	0	0	no channel selected; power-up/reset default state

Figure 36: Multiple channel selection for PCA 956A.

Can be selected and deselected at the same time after a STOP condition has been placed on the Bus. For example, when B3= 0, B2 = 1, B1=1 and B0=0, channel 1 and 2 are enabled and at the same time channel 0 and 3 are disabled.

The I2C bus characteristics for PCA 9546A is same as PCA 9505 for Bit Transfer, START and STOP conditions, System configuration and Acknowledgement. So they are omitted here.

4.2.3.4. Reading and writing on the Control Registers (Bus Transaction):

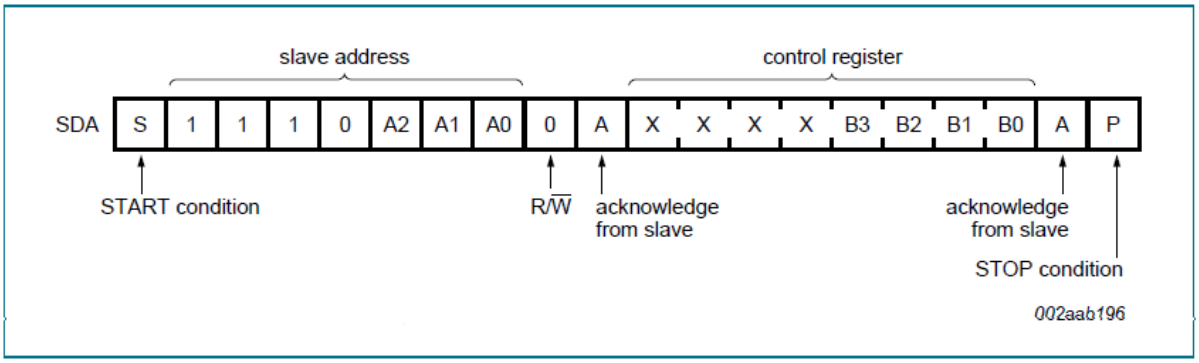

Figure 37: Write operation in PCA 9546A Control Register.

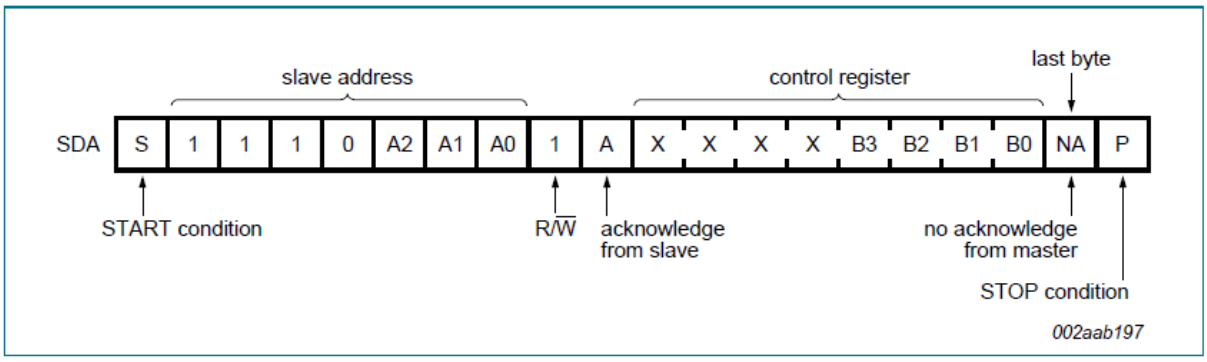

Figure 38: Read from PCA 9546A Control Register.

4.3. SOLID Hardware Interface:

```
#ifndef __SOLID_H
#define __SOLID_H
#include "stdint.h"

#define OUTPUT 0x00
#define INPUT  0xFF

#define HIGH  0x01
#define LOW   0x00

#define SOLID_I2C I2C_IDX2

#define PCA9505_ADDRESS  0x20
#define SWITCH_PCA9546A_ADDRESS          0x70


uint8_t Switch_PCA9546A(uint8_t Channel);
uint8_t Read_Port(uint8_t Port_Type, uint8_t Port_Number);
uint8_t Config_Port(uint8_t Port_Number, uint8_t Status);
uint8_t Read_Pin(uint8_t Port_Type, uint8_t Port_Number, uint8_t
Pin_Number);
uint8_t Write_Pin(uint8_t Port_Number, uint8_t Pin_Number, uint8_t
Pin_Value);

#endif
```

4.4. SOLID working principle:

Swich PCA 9546A is able to select and deselect any of those three IO Expander (PCA 9505) through I2C command from the Microcontroller. A total of 30 x 30 input and output ports are associated in the SOLID electronics. All the 30 diagonal lines are known as detector lines, meaning, primarily, the detector line will read from the telemetry data, whether there is an impact or not. To find the exact Cartesian coordinate on the panel, the scanning algorithm is applied. The scanning is divided into two triangles. The upper triangle will detect impact position and location for the Axes X1 - Y2. In broader sense, the total area for (X1-1, X1-2, X1-3 and Y2-1, Y2-2, Y2-3). Similarly the lower triangle portion will detect impacts through the ports those are defined in the Cartesian coordinate X2-Y1 (X2-1, X2-2, X2-3 and Y1-1, Y1-2, Y1-3).

The same scanning algorithm applies for all the eight panels of the TechnoSat. Each panel is associated to a panel ID which can be send and retrieved from the Tele command and Telemetry data. Without an impact, all the output pins should give a value ‘1’ as readout value and a telemetry data is obtained from each panel will be stored and downloaded in a 30x30 Matrix format. This is rather raw data. The detector lines (diagonal pins) are scanned first, and the output pin value is checked, when there is an impact, the corresponding detector line should give an output value ‘0’ to the corresponding pin on PCA 9505 chip. This value is then stored, scan continues until all the detector lines are read for output values. In the next step, the algorithm checks for the corresponding X-Y Cartesian position. Which is also saved as part of the Matrix data and retrieved on the Ground Station for further analysis. If multiple hit occurs in the same SOLID panel and in the same position, this would not be detected as multiple impacts.

Since, TechnoSat is still waiting to be launched with its other payloads, a real and on orbit Telemetry data is not available to demonstrate the functionality of SOLID hardware. But A simulated Graphical User interface has been created in order to explain how it will function. For this, the prototype circuit has been used to read out the data from a SOLID panel. Some artificial discontinuities have been imposed on the prototype electronics, as if the Panel has been hit by some debris. These are our Test Case Scenario.

In the next chapter, the GUI (Graphical User Interface) Environment will be discussed broadly and the Test case scenarios will be presented as Ground Observation and user realization for Debris in a Particular Orbit.

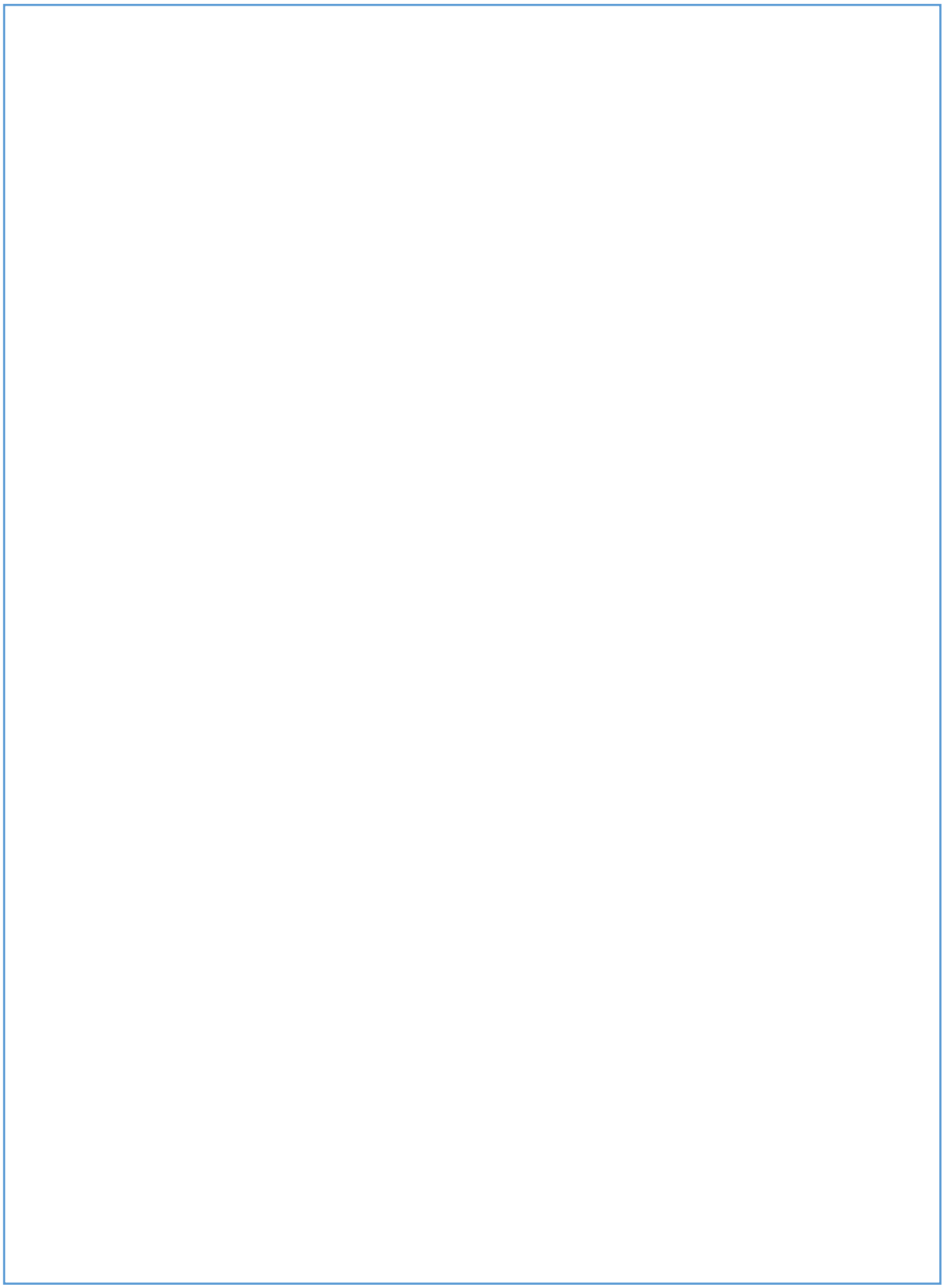

Figure 39: Solid hardware electronics TOP view.

Figure 40: IO-Expander (PCA 9505) and I2C switch (PCA 9546A) layout for the SOLID electronics.

Figure 41: The Impact detector area; IO-Expander input and output lines in a matrix.

5. Results and Discussions

5.1 Particle Flux and impact probability:

As mentioned earlier, TechnoSat is an octagonal shaped satellite with a maximum dimension of 300 x450 x450 mm. Allowing the satellite to fly in the orbit, the maximum Ram direction will be exposed can be considered as an area of a rectangle; which is 300 x 450 mm^2. Or 0.135 m^2.

As we know that the theoretical impact particle flux density can be given as:

$$Impact\ Particle\ Flux\ Density = \frac{Number\ of\ Hits}{Exposed\ Spacecraft\ Area\ \times Time\ in\ Year}$$

Considering an optimal statistics of Debris particle density in the LEO and an exposure time of one year, the Number of theoretical impacts on Technosat Ram Side would be:

$$Number\ of\ Impacts\ in\ one\ year\ for\ 3mm\ particle\ = 0.135m^2 \times 2.2610^{-4}\ hits\ m^{-2}$$
$$= 1.710\ Hits$$

$$Number\ of\ Impacts\ in\ one\ year\ for\ 9mm\ particle\ = 0.135m^2 \times 2.2610^{-5}\ hits\ m^{-2}$$
$$= 1.585\ Hits$$

Which suggests that, Technosat will experience some Impacts on the SOLID panel. Since the above statistics is based on the trackable objects by different other methods, and the values are only a good estimations by some Authors [53], the real impact scenario in orbit will be more than the calculated values. Since, many particles are undetected and the aim for SOLID is to detect impacts by in situ measurements. In addition to that, there will also be some impacts on the Wake side of Technosat.

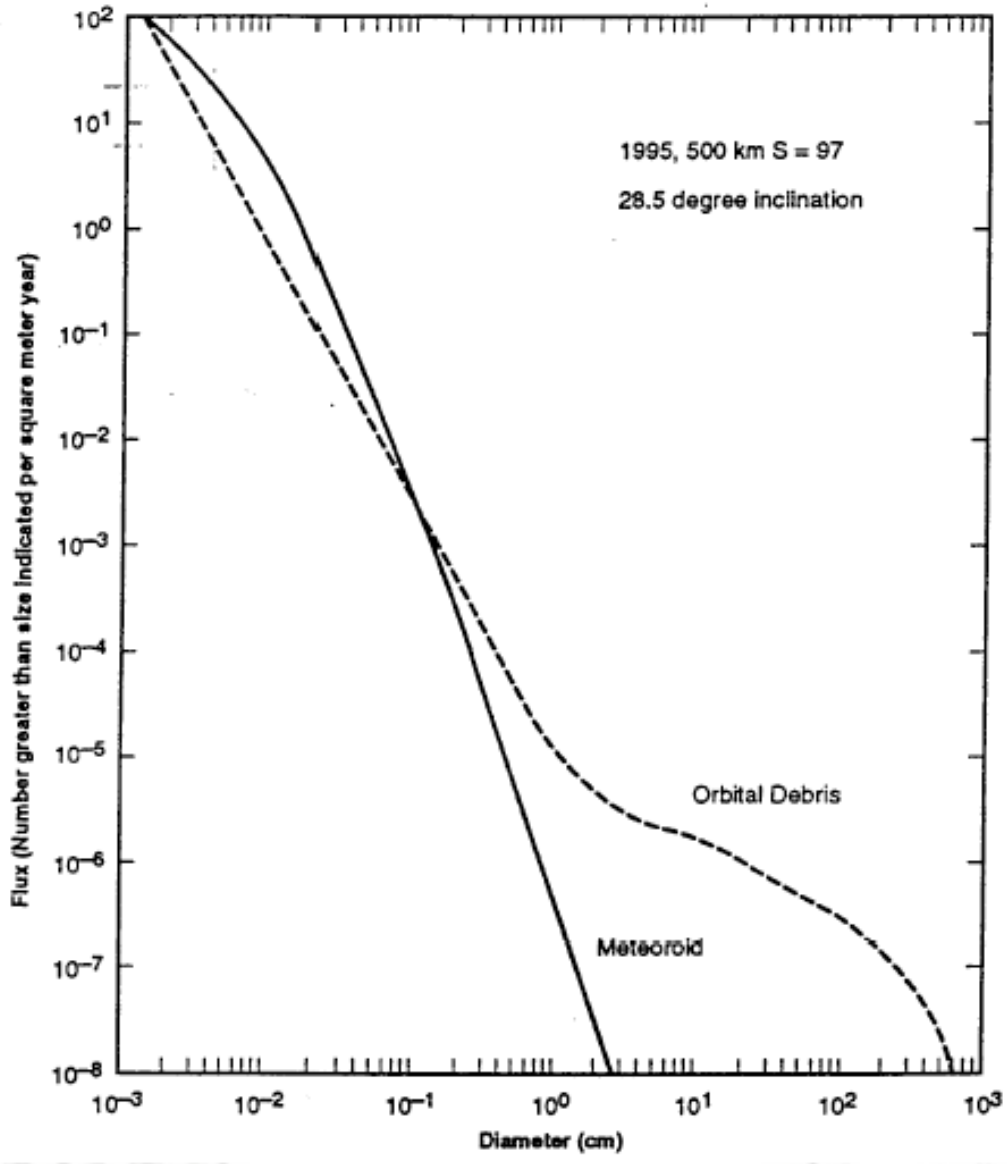

Figure 42: The Particle Flux Density vs the Particle Size. [53]

5.2 Telemetry Data and QT Simulator Application:

Since we do not have a real Telemetry (TM) data for the time being, the impacts or debris hits on the SOLID panels will be generated here using a randomly generated hit counts by means of a Text file. The Text file is an efficient and convenient way to represent the simulated data as a Matrix format which is used by the simulator program as an Array. It is worth mentioning that, the real telemetry data at the downlink will not be received as a Text file, rather it would be some sort of other Raw Data format. The conversion of this data format to a Text file or to conversion of the input data stream to the simulator has been left alone under Future Work.

The work flow of the simulator starts off with the reception of the Telemetry data which contains the panel Matrix. The panel Matrix is nothing but a collection of 0's and 1's and represents a 30 x 30 Matrix. This specification has been discussed in the SOLID Electronics section. The main program then checks for the received data format, when the data format is read as a *.txt file, the data stream is read. In other words, the file is read till the end and the data are parsed to the QT program to generate the Graphics. The program will terminate automatically when the input file format does not comply with the above specification.

The Main graphics window is run or generated after the data has been read and parsed successfully. The GUI initializes the panel view, an image of the satellite, an updating view of the TLE (Two line Elements) for Technosat, an option to go back and forth to see all the panels with the current impact situations and particle hits represented by small circles or ellipses. A work flow diagram of the entire simulator is presented in the next page with some block specifications and explanations.

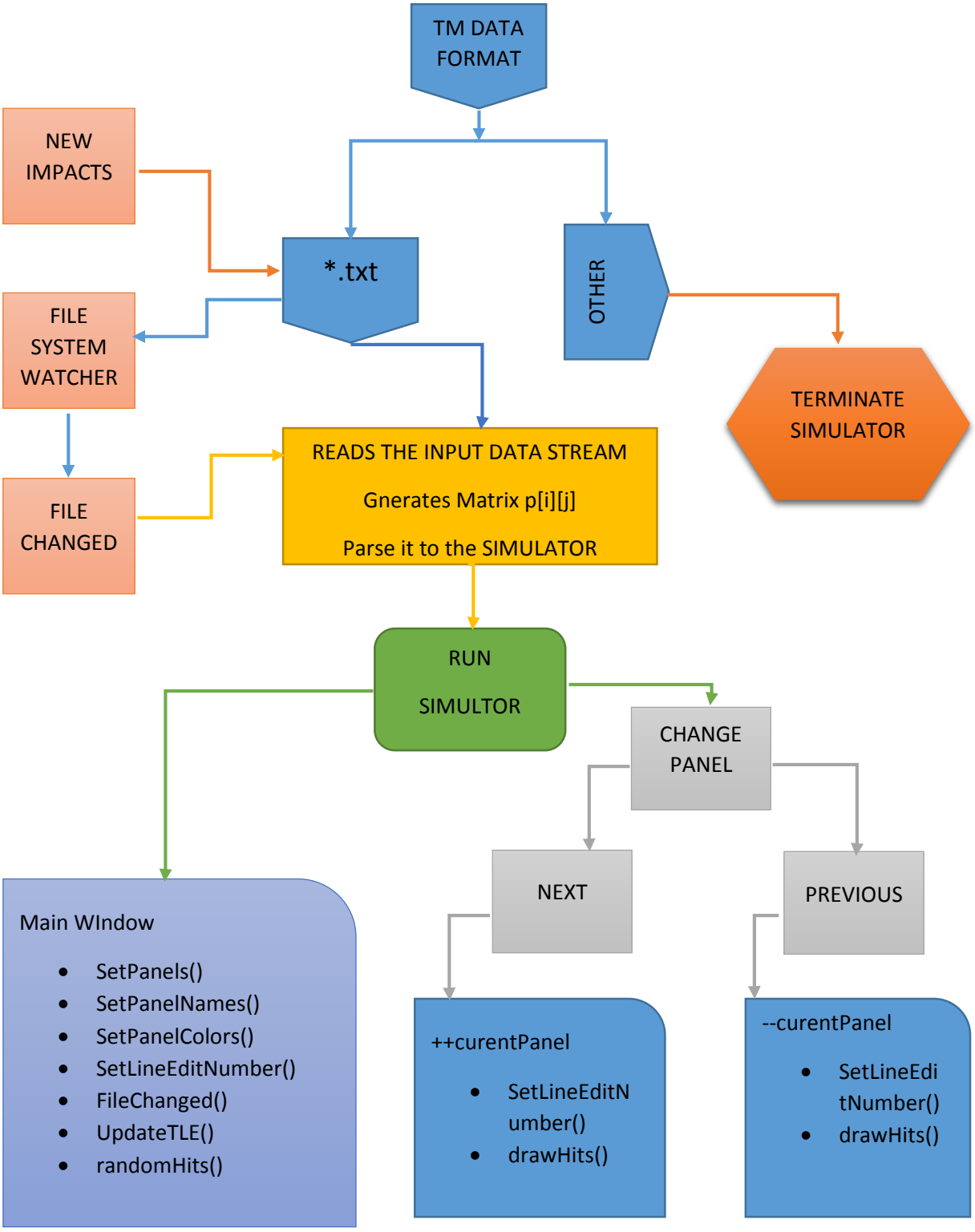

Figure 43: SOLID simulator Flow diagram.

It is also worth mentioning the main blocks of the simulation procedure and the different execution levels:

MainWindow()

- Initiates the current panel, N(N=1-8).
- Changes the Two Line Elements (TLE).
- Generates the Random Hits on the panel.
- Also adds the satellite image for Technosat.

SetPanels()

- Removes the Old Panel and writes a new one.
- Holds the current panel counter and
- Draws the Hits.

FileChanged()

- Opens the TM data file (*.txt).
- Reads the entire file and copies new Panel Array, colors then draws Hits.

SetLineEditNumber()

- Removes previous Hits on each panels
- Draws new hits for each panel

randomHits()

- For each and every panel randomly picks a cartesian position on the panel and drwas Hits without replacing the previous ones.

Update TLE()

- Updates the Two Line Elements fort he Satellite

drawHits()

- Delete all items apart from the last circular dots on the panel.

5.3 Simulated Results:

Test Case were created using the output pins readings using the SOLID prototype Hardware electronics. The Test Case scenarios represents the Telemetry data after the panels are scanned in orbit. Whenever an impact occurs on the panel, the corresponding Telemetry Data file will be updated and will be stored in the memory. As well as the position of the impact, other orbital elements can also be obtained to obtain the impact position in the orbit. The GUI has been implemented using Qt GUI developer, which is a C++ platform. This is the regular GUI look before any hit occurs on any of the SOLID panels:

When the QT application is executed, the simulator generates the GUI which represents the current SOLID panel and the status of the panel in terms of Particle Impacts. The Matrix box on the far left side represents the panel, in this case this is panel one. On the top right, there is the 'Two Line' elements for satellite tracking (TechnoSat). The different panels can be selected by using the 'Next' and 'Previous' buttons. The bottom right corner is the actual image of TechnoSat satellite.

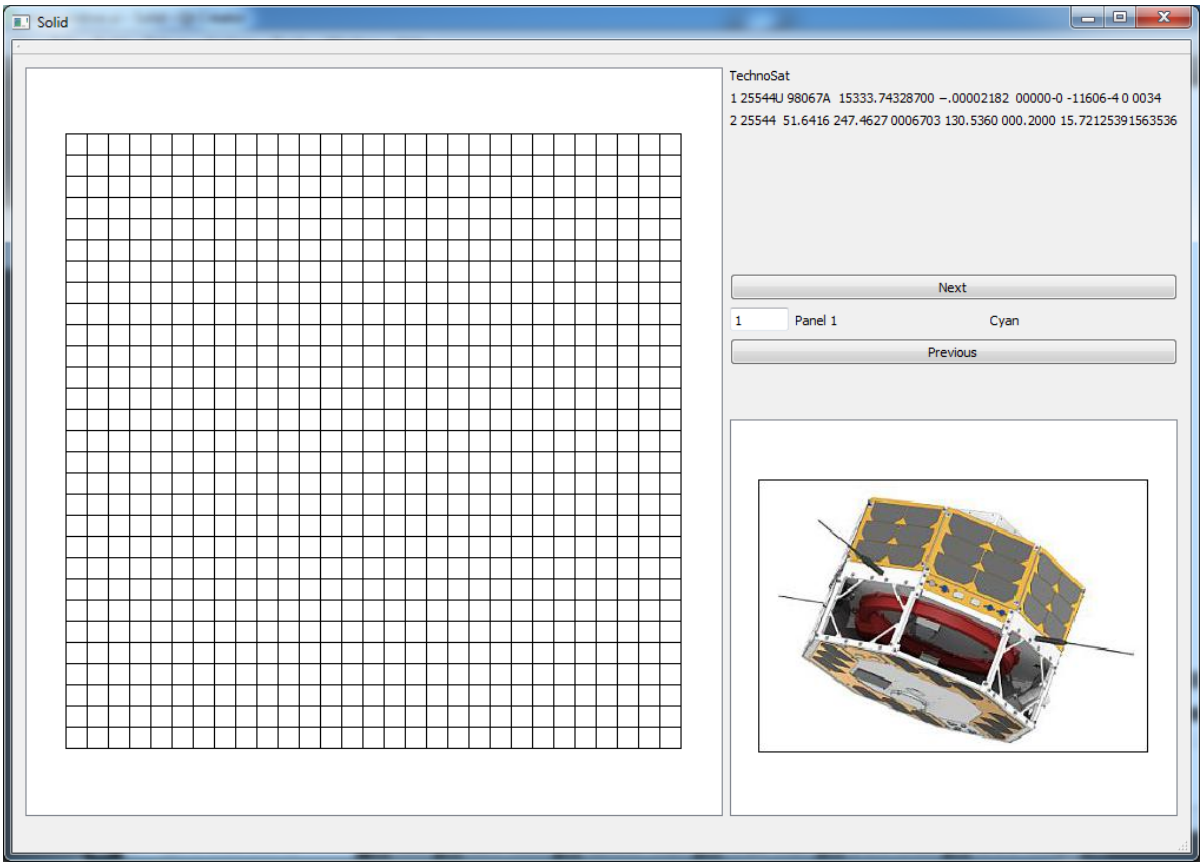

Figure 44: GUI representation of SOLID panel on Ground station without any impact.

As, the satellite makes more and more passes, after it has been placed in the orbits, it detects more and more debris and impacts. The corresponding Telemetry Data File will be updated accordingly. The following simulations show impact growing as the satellite spends more time in Orbit. Figure 43-45.

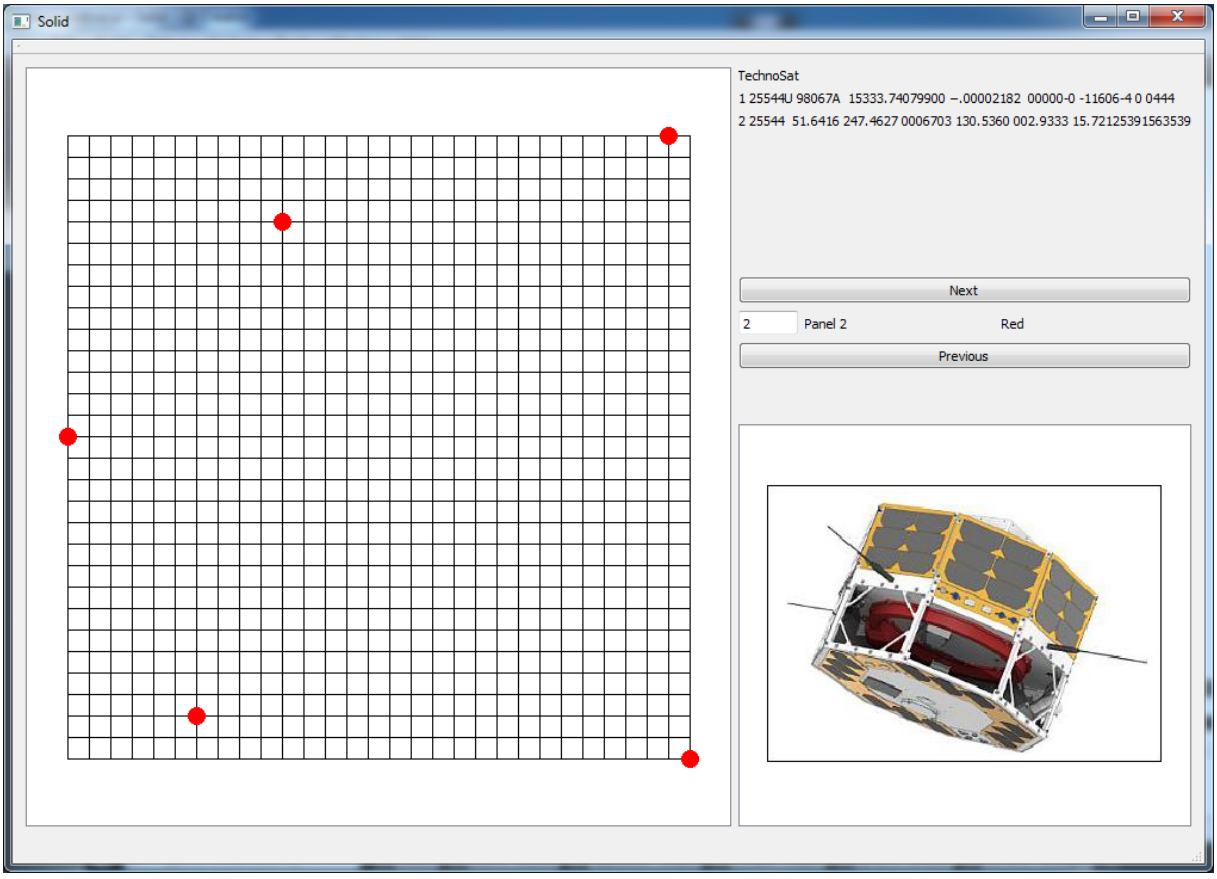

Figure 45: The first few impact has been detected on TechnoSat SOLID panel 2.

Similarly, the other panels show the simulation results in an efficient way. Impact detections from panel 5, 6 and 8 have been included in Figure 46-48. All the panels (1-8) are simulated for the Test Case Scenario and they are generating expected results for the corresponding best case.

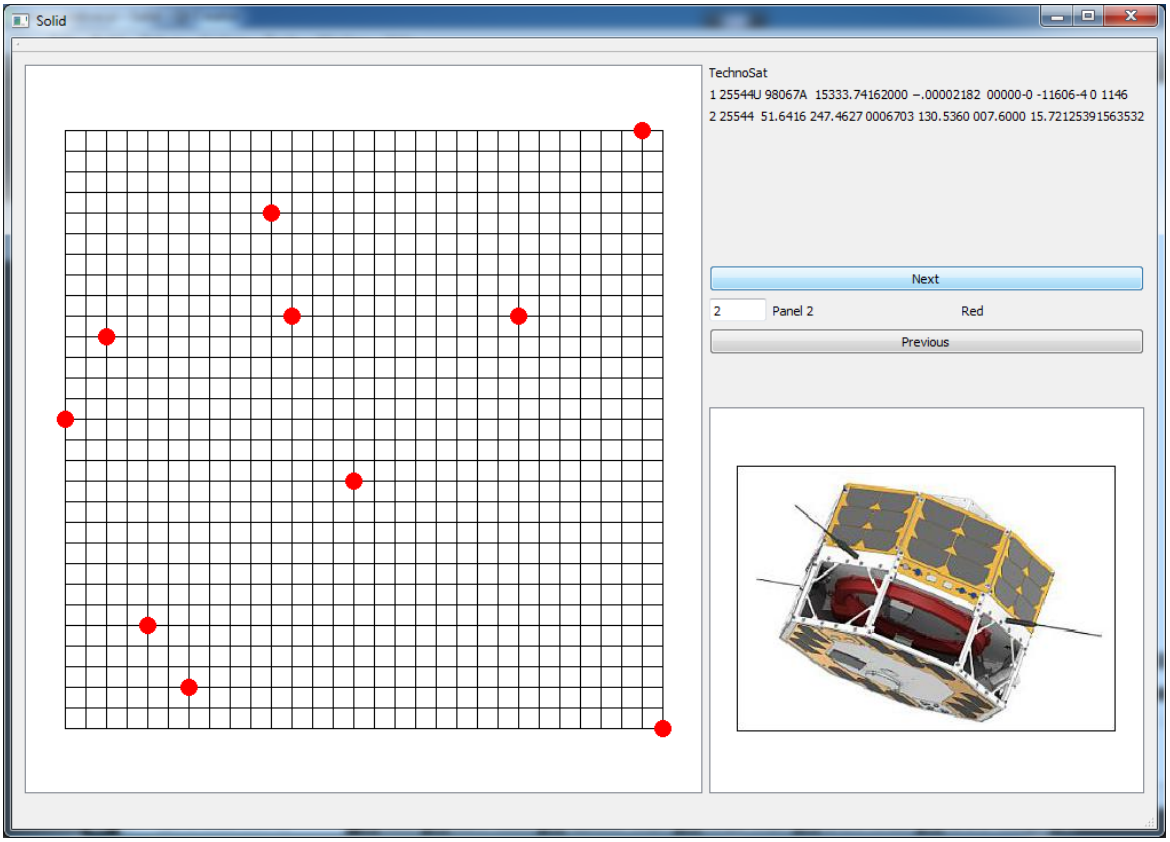

Figure 46: SOLID panel 2 with after more impacts.

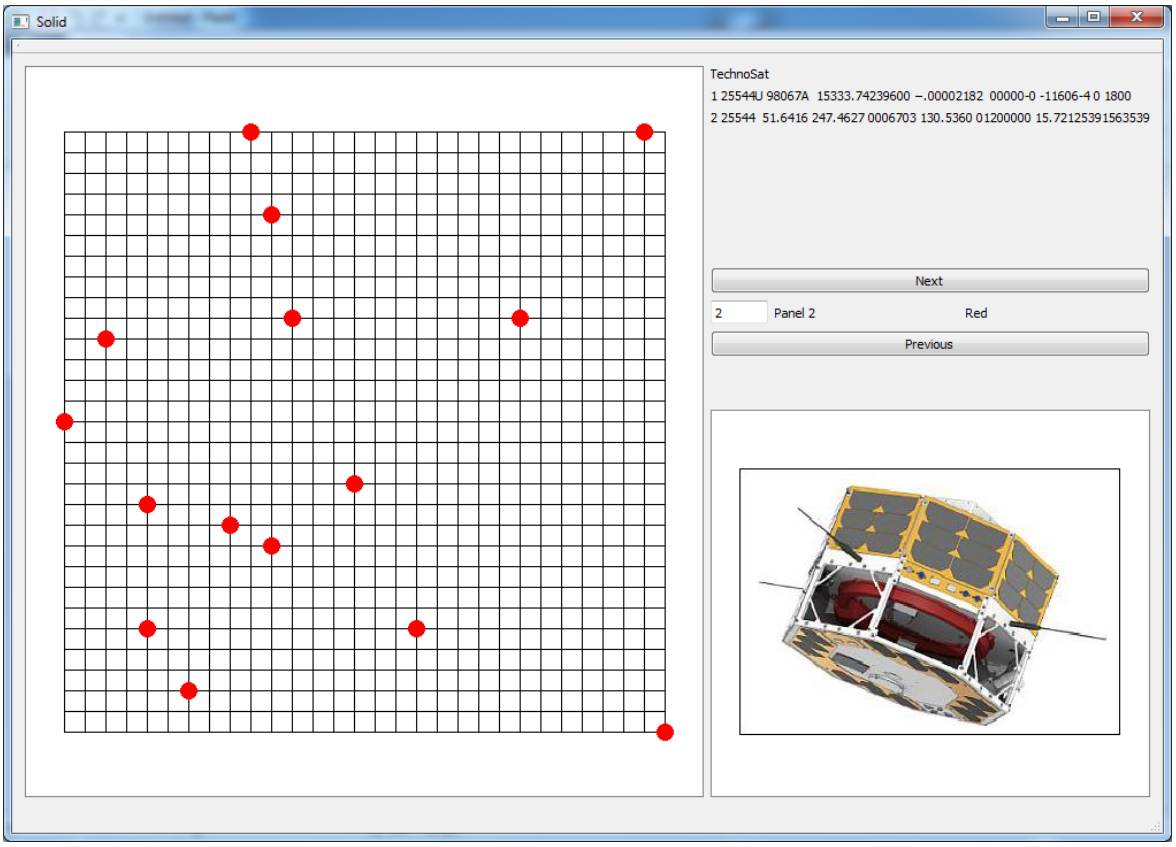

Figure 47: SOLID panel 2 impact gathering in continuous time.

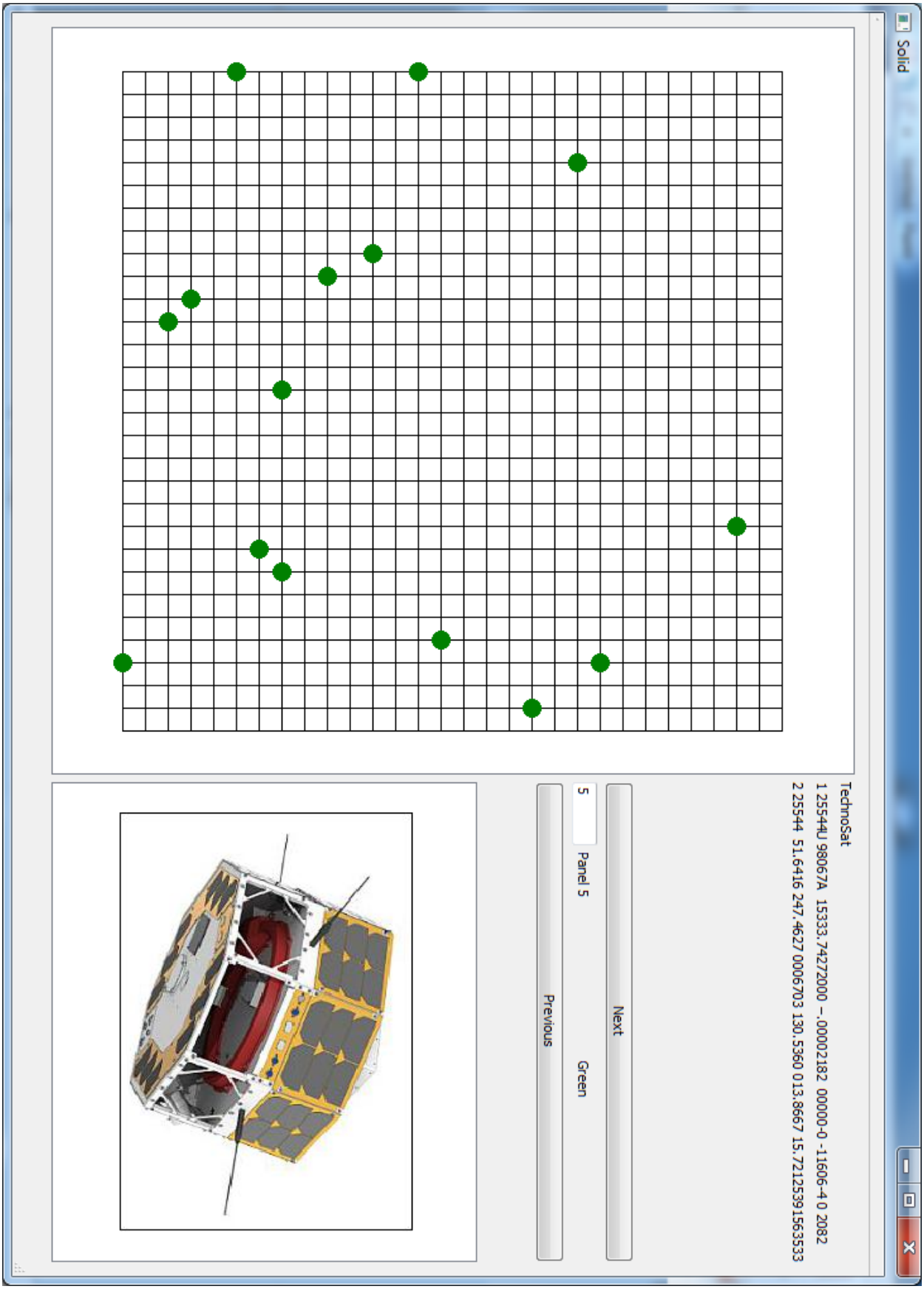

Figure 48: SOLID panel 5 impact with detected impacts.

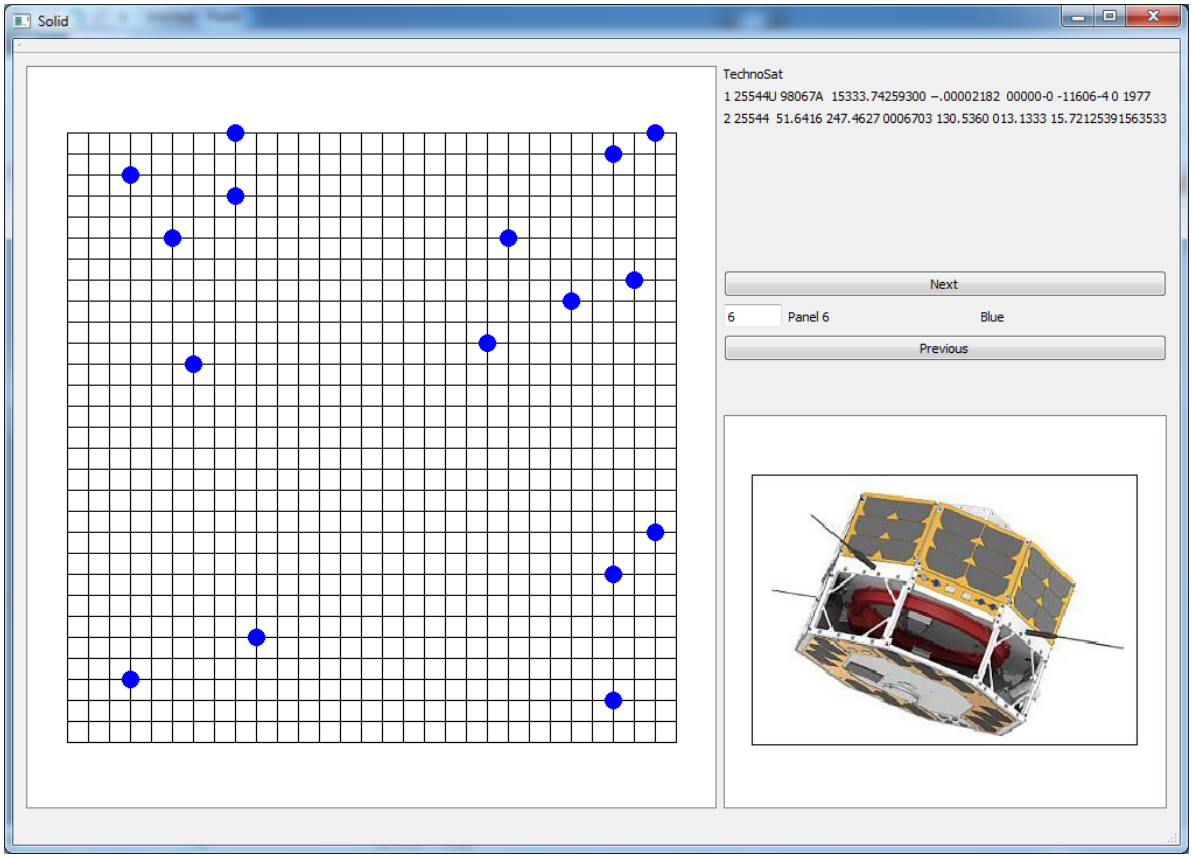

Figure 49: SOLID panel 6 impact with detected impacts.

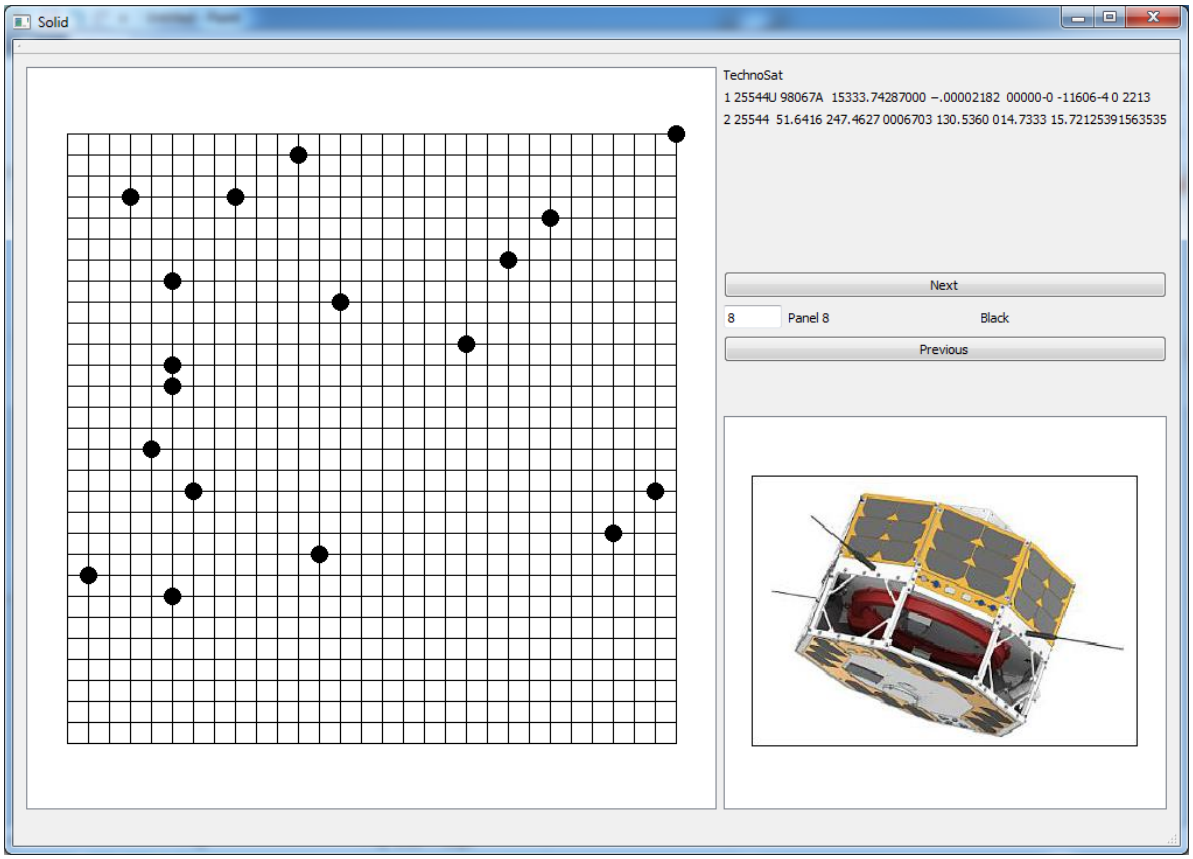

Figure 50: SOLID panel 8 impact with detected impacts.

6. Conclusion and Future Work :

In-situ observation to detect and map millimeter sized Space Debris is both an efficient and economic approach on board a nanosatellite. Since, the retrieval of space hardware is quite expensive and time consuming, depending on the mission. But SOLID will be flying as a Secondary payload can generate a useful map about debris in the corresponding mission orbit. The Interfacing was done in an efficient manner in order to gain less processing power, less memory occupation and lesser power consumption. The GUI was designed in such way, that it can generate and update the mapping of impacts autonomously using the Telemetry data that is very helpful to visualize the impacts from the Ground as an alternative of retrieval of SOLID hardware.

TechnoSat is still waiting to be launched. The impact detector electronics has been changed and modified quite a few times to make it better. The Hardware Interfacing needs to be included with the main satellite software module. And finally, GUI needs to be integrated with the Ground Station software for continuous update of the impact mapping. After the exact orbital position of Technosat is known, the Orbitl elements will be helpful to generate some kind of 3D model of particle density in the GUI.

Also worth mentioning the fact as discussed earlier, the real telemetry data needs some sort of modification to generate the mapping of the corresponding debris impact on the Ground segment visualizer. Also, more in case of multiple hits on a single position on the SOLID panel will only detect as a single impact. A bigger impact followed by smaller impacts will only detect the first and larger impact.

7. Refernences:

[1] Cheng, B (1997). *Studies in International Space Law*. Oxford: Clarendon Press. p396-397.

[2]Hastings, D and Garrett, H (2004). *Spacecraft-Enironment Intraction*. Cambridge: Cambridge University Press. p108-109.

[3]Lu,E.(2003).*FutureSpaceships.*Available:http://spaceflight.nasa.gov/station/crew/exp7/luletters/lu_letter8.html. Last accessed 21th Nov 2015.

[4] Hastings, D and Garrett, H (2004). *Spacecraft-Enironment Intraction*. Cambridge: Cambridge University Press. p70-82.

[5] Holli Riebeek. (2009). *Catalog of Earth Satellite Orbits.* Available: http://earthobservatory.nasa.gov/Features/OrbitsCatalog/. Last accessed 21th Nov 2015.

[6] Vincent L. Pisacane (2005). *Fundamentals of Space Systems*.

[7] Vallado, D (2013). *Fundamentals of Astrodynamics*. 4th ed. Hawthorne, CA: Microcosm and Springer. p41- 104.

[8] Vallado, D (2013). *Fundamentals of Astrodynamics*. 4th ed. Hawthorne, CA: Microcosm and Springer. p150- 154.

[9] Klinkrad, H (2006). *Space Debris Models and Risk Analyis*. Chichester, UK: Praxis Publisching Ltd.. p1-3.

[10] Weeden, B. (2009). *What's in Earth orbit and how do we know?*. Available: http://www.thespacereview.com/article/1417/1. Last accessed 21th Nov 2015.

[11] Klinkrad, H (2006). *Space Debris Models and Risk Analyis*. Chichester, UK: Praxis Publisching Ltd.. p5-15.

[12] NASA. (2014). Spatial Density. *Orbital Debris Quarterly News*. 18 (2), p1-10.

[13] NASA. (2014). Spatial Density. *Orbital Debris Quarterly News*. 18 (1), p1-10.

[14] NASA. (2015). Spatial Density. *Orbital Debris Quarterly News*. 19 (2), p1-10.

[15] ESA. (2013). *Mitigating space debris generation.* Available: http://www.esa.int/Our_Activities/Operations/Space_Debris/Mitigating_space_debris_generation. Last accessed 21th Nov 2015.

[16] NASA Orbital Debris Program Office. (2010). *Orbital Debris Shielding.* Available: http://orbitaldebris.jsc.nasa.gov/protect/shielding.html. Last accessed 21th Nov 2015.

[17] NASA. (2014). Spatial Density. *Orbital Debris Quarterly News*. 19 (3), p1-10.

[18] NASA. (2014). Spatial Density. *Orbital Debris Quarterly News*. 19 (1), p1-10.

[19] Kushner, D. (2010). Cluttered Space. *Popular Science*. 2(8), p60-64.

[20] Ariyoshi, Y, Kashima, S, Hanada, T, Kitazawa, Y and Kawabe A. (2011). *Effectiveness of Passive Orbital Debris Removal for Future Environment.* Available: http://archive.ists.or.jp/upload_pdf/2011-r-38.pdf. Last accessed 21th Nov 2015.

[21] Michaels, D. (2011). *A Cosmic Question: How to Get Rid Of All That Orbiting Space Junk?.* Available: http://www.wsj.com/articles/SB123672891900989069. Last accessed 21th Nov 2015.

[22] Bekey, I (1997). *Project Orion: orbital debris removal using ground-based sensors and lasers*. In Second European Conference on Space Debris, page 699, ESA SP-393.

[23] Campbell, J W. (2000) *Using Lasers in Space: Laser Orbital Debris Removal and Asteroid Detection*, volume 20. Center for Strategy and Technology, Air War College, Air University Maxwell Air Force Base, Alabama.

[24] Bombardelli,C and Pelaez, J. (2010). Ion beam shepherd for contactless space debris removal.. Journal of Guidance, Control and Dynamics. 34 (3), p916-920.

[25] Mehrholz,D.(1995). *"Radar detection of mid-size debris," Adv. Sp. Res.*16 (11), p17–27.

[26] Mehrholz,D.(2001). *"Radar techniques for the characterization of meter—sized objects in space,"* Adv. Sp. Res., 28(9), p1259–1268.

[27] Bai, X, Xing, M, Member, A, Zhou, F, Bao, Z and Member, S. (2009*.) "High-Resolution Three Dimensional Imaging of Spinning Space Debris,"* 47(7), p2352–2362.

[28] Sato,T. (1999) *"Shape estimation of space debris using single-range Doppler interferometry,"* IEEE Trans. Geosci. Remote Sens, 37(2), p1000 –1005.

[29] Hong,L Dai, F and Liu, H. (2013*) "Sparse Doppler-only snapshot imaging for space debris,"* Signal Processing, 93(4), p731–741.

[30] Africano, J, Stansbery, E and Kervin, P (2004) *"The optical orbital debris measurement program at NASA and AMOS,"* Adv. Sp. Res., 34(5), p892–900.

[31] Kervin, P. W, Africano, J. L, Sydney, P. F and Hall, D. (2005) *"Small satellite characterization technologies applied to orbital debris,"* Adv. Sp. Res. 35(7), p1214–1225.

[32] Hall,D , Hamada, K, Kelecy, T and Kervin,P. (2012) *"Surface Material Characterization from Non-resolved Multi-band Optical Observations,"* in Advanced Maui Optical and Space Surveillance Technologies Conference.

[33] Schildknecht, T, Musci, R and Flohrer, T.(2008) *"Properties of the high area-to-mass ratio space debris population at high altitudes,"* Adv. Sp. Res., 41(7), p1039–1045.

[34] Schildknecht, T, Früh, C, Herzog,J, Hinze, A and Vananti, A.(2010). *"AIUB EFFORTS TO SURVEY, TRACK, AND CHARACTERIZE SMALL-SIZE OBJECTS AT HIGH ALTITUDES,"* in Advanced Maui Optical and Space Surveillance Technologies Conference.

[35] Lambert, J.V, Osteen, T. J and Kraszewski, W. A. (1993). "*Determination of debris albedo from visible and infrared brightnesses,"* in *Space Debris Detection and Mitigation.*, 1951, p32–36.
[36] Hejduk, M. D, Cowardin, M. D and Stansbery, E. G (2012). *"Satellite Material Type and Phase Function Determination in Support of Orbital Debris Size Estimation,"* in Advanced Maui Optical and Space Surveillance Technologies Conference.

[37] Oswald, M, Krag, H, Wegener, P and Bischof, B.(2004) *"Concept for an orbital Telescope observing the debris environment in GEO,"* Adv. Sp. Res., 34(5), p1155–1159.

[38] Flohrer, T, Schildknecht, T and Musci, R.(2008.) *"Proposed strategies for optical observations in a future European Space Surveillance network,"* Adv. Sp. Res., 41(7), p1010–1021.

[39] Skinner, M.A, Russell, R. W, Rudy, R. J, Gutierrez, D. J, Kim, D. L, Crawford, K, Gregory, S and Kelecy, T (2011) *"Time-resolved infrared spectrophotometric Observations of high area to mass ratio (HAMR) objects in GEO,"* Acta Astronaut.,69(11-12), p1007–1018.

[40] Skinner, M. A, Russell, R. W, Kelecy, T, Gregory, S, Rudy, R. J, Gutierrez, D. J,Kim, D. L and Crawford, K (2012) *"Further analysis of infrared spectrophotometric observations of high area to mass ratio (HAMR) objects in GEO,"* Acta Astronaut.,80, p154–165.

[41] Gaposchkin, E. M and Bergemann, R. J (1995*). "Infrared Detections of Satellites with IRAS,"* in MIT Lincoln Laboratories Space Control Conference.

[42] Dawson, J. A and Bankston, C. T (2010). *"Space debris characterization using thermal imaging systems,"* in Advanced Maui Optical and Space Surveillance Technologies Conference.

[43] Harms, A, Hamada, K, Wetterer, C. J, Luu, K, Sabol, C and Alfriend, K. T (2011). *"UNDERSTANDING SATELLITE CHARACTERIZATION KNOWLEDGE GAINED FROM RADIOMETRIC DATA,"* in Advanced Maui Optical and Space Surveillance Technologies Conference.

[44] Kervin, P. W, Africano, J. L, Sydney, P. F and Hall, D(2005) *"Small satellite characterization technologies applied to orbital debris,"* Adv. Sp. Res., 35(7), p1214–1225.

[45] Klinkrad, H (2006). *Space Debris Models and Risk Analyis*. Chichester, UK: Praxis Publisching Ltd.. p47-57.

[46] Institute of Aeronautics and Astronautics. (2015). *TechnoSat.* Available: http://www.raumfahrttechnik.tuberlin.de/menue/research/current_projects/technosat/parameter/de/. Last accessed 21th Nov 2015.

[47] Merlin, F; Frank, B; Walter, B; Karsten, G; Christian, N and Klaus, B (2013). *" TUBiX20 - The novel Nanosatellite Bus of TU Berlin. "* Proceedings of the 9th IAA Symposium on Small Satellites for Earth Observation, p93-96.

[48] Noack, D; Jonathan, L and Brieß, K (2014). *"Fluid-Dynamic Attitude Control Experiment for TechnoSat."* The ESA/CNES Small Satellites Systems and Services (4S) Symposium.

[49] Merlin F.B; Karsten, G and Sergio, M (2014). *"Implementation of a Nanosatellite On-Board Software based on Building-Blocks"*. The ESA/CNES Small Satellites Systems and Services Symposium.

[50] Cook, N P (1999). *A First Course in Digital Electronics*. Upper Saddle River, NJ: Prentice Hall. p1-814.

[51] Wright, D (2010). *The Current Space Debris Situation*. Orbital Debris Mitigation Workshop, Beijing, China.

[52] NASA's Orbital Debris Program Office: Briefing to the NASA Advisory Council.

[53]Tribble, A (1995). *The Space Environment: Implications for Spacecraft Design*. Princeton: Princeton University Press.